

# Reducing Recurrent Competitive Epidemics via Dynamic Resource Allocation

Argyris Kalogeratos, Gaspard Abel, Stefano Sarao Mannelli

**Abstract**—Motivated by scenarios of epidemic competition, as well as how social contagions spread at the level of individuals, this work considers the competition between two conflicting node states that spread over a social graph according to a generic diffusion process. For this setting, we introduce the *Generalized Largest Reduction in Infectious Edges* (gLRIE), which is a dynamic resource allocation strategy that favors the preferred state against the other. Our analysis assumes a generic continuous-time SIS-like (Susceptible-Infectious-Susceptible) diffusion model that allows for: arbitrary node transition rate functions for nodes to change state, and competition between the healthy (positive) and infected (negative) states, which are both diffusive at the same time, yet mutually exclusive at each node. The strategy follows a *minimum-risk-maximum-gain* principle, and its features are particularly relevant for social contagion phenomena. In accordance with the LRIE strategy that we generalize, we show that in this context the gLRIE strategy remains a greedy solution for the minimization of the number of infected network nodes over time. Ultimately, simulations are employed to compare the proposed strategy with other existing alternatives, demonstrating that gLRIE exhibits superior performance across a spectrum of scenarios, including a realistic counter-contagion campaign in a small well-monitored community.

**Index Terms**—Competitive spreading processes, social contagions, behavioral epidemics, epidemic modeling, agent-based models, epidemic control, dynamic resource allocation, contact networks.



## 1 INTRODUCTION

**D**IFFUSION processes are being studied since the last century, for obtaining models that could help us understand and predict real-world phenomena. In recent years, the growing amount of available network data led to a surge in the application of diffusion processes, and yielded to a plethora of refined models that are closer to reality. Diffusion models are used in disparate branches of science: economics (competition among products [1], viral marketing campaigns [2]), epidemiology (disease spreading [3], vaccination [4], [5] and allocation of medical resources [6], [7], [8]), computer and information science (propagation of rumors [9], [10], [11], [12], and computer viruses [13]).

In these last decades, the increasing quantity of data gathered in networked socioeconomic studies has generated a novel field of interest to statisticians, sociologists and physicists. Their approach stems from the idea that various complex social behavior phenomena can be represented and interpreted as *social contagions* [14] that a network of agents can adopt and transmit when via contact with its neighborhood. Notable examples are: human emotions [15], behaviors pertaining to public health issues such as obesity diffusion [14], [16], smoking cessation [17], [18], alcohol abuse [19], drug use [20], [21] or other related to wrongdoing [22], [23].

Due to the diffusive nature of such behaviors, adaptive network-level strategies outperform alternatives that are limited to individual-level interventions. This is why researchers, public

health professionals, and policy makers should investigate how to leverage social-network-level information to optimize the efficacy of counter-contagion interventions.

Many of the above examples correspond to behavioral epidemics with recurrent effects, allowing reinfections, as permanent immunity is never achieved. The Susceptible-Infected-Susceptible (SIS) [24] model is a good basis to study such epidemics, yet it is deemed simple to describe several real-world phenomena. While several SIS extensions have been developed, we briefly describe a selection of the ones most relevant to the aim of this work. In terms of model granularity, as opposed to the coarse-grained compartmental models [25], [26], agent-based models (ABMs) provide a framework for high-resolution node interaction. In this setting a node can become infected according to a transition rate that is *linear* and *local*: i.e. the change of a node's state is a stochastic function that depends linearly on the states of its neighbors, hence depicting a social influence effect. Yet, the assumption for linear infection rates can be restrictive for problems where, for example, the response of individuals exhibits saturation effects [27]. A number of studies have provided evidence supporting the need for more complex transition rate functions to better mimic real-world processes, e.g. as in the SISa model [14], [15]. Most such epidemic models consider the infected state to be the only one that diffuses, however, in the context of behavioral epidemics, it is natural to consider that social influence spreads both negative and positive attitudes. As a matter of fact, social norms emerge from the observation of the conduct of influential contacts, the adoption and then the emulation of these behaviors, which disseminates them further to others [22], [23], [28].

Across the spectrum of the above application domains, modeling efforts raise questions about how to reduce an undesirable diffusion. This line of research has offered numerous intervention techniques (see [29] for a survey). Two standard approaches to control an epidemic process is *vaccination* (administration of

• A.K. and G.A. are with the Centre Borelli, ENS Paris-Saclay, CNRS, Gif-sur-Yvette, France. G.A. is also with the Centre d'Analyse et de Mathématique Sociales, EHESS, CNRS, Paris, France. S.S.M. is with Data Science and AI, Computer Science and Engineering, Chalmers University of Technology and University of Gothenburg, Gothenburg, Sweden, and the School of Computer Science and Applied Mathematics, University of the Witwatersrand, Johannesburg, South Africa.

• Correspondence to: A.K.; email: argyris.kalogeratos@ens-paris-saclay.fr.

Manuscript received December XX, XXXX; revised XXXX XX, XXXX.

medicines to specific nodes) and *quarantine* (modification of the network structure by deleting a set of edges). Most of these strategies are *static* and are based on the network structure, e.g. the work in [30] or the greedy algorithm to reduce the spectral radius of a graph from [31]. Additionally, the problem of nonlinear infection rates between nodes is investigated in [32], where a heuristic is devised for blocking the epidemic spread. There are also *dynamic* strategies that use information about the current state of the network to suggest the best nodes to treat [6], [33], [34], [35]. Among them, the *Largest Reduction in Infectious Edges* (LRIE) [34] is a greedy algorithm for resource allocation to control SIS epidemics with a limited budget, and is the main source of inspiration for this work.

Alternately, literature in social network analysis has also raised interest in studying social contagion. Namely, opinion dynamic models exhibit similar properties to competitive epidemic models considered here, and optimal strategies to promote a desired state can be as well relevant. Theoretical results on threshold and voting models [36], [37], [38] propose an optimal intervention strategy to influence the innate opinion of social network agents. Additionally, the epidemic dynamics can also be tackled with a Temporal Point Processes, which rely on probabilistic interaction models. To this end, stochastic optimal control frameworks have been introduced to mitigate the spread of an epidemic [39], [40], or to increase user interaction in social networks [41].

The above discussion makes evident that, on the one hand, the literature on modeling one or multiple network diffusion processes has brought a variety of results, including optimal control strategies, while on the other hand, the use of ABMs for the analysis of diverse diffusing social behaviors has gained considerable attention as it could lead to local interventions to facilitate establishing a desired social norm.

**Contribution.** We present the *Generalized Largest Reduction in Infectious Edges* (gLRIE), a score-based dynamic resource allocation framework for controlling competing recurrent diffusions, seen as Markov processes with arbitrary functions describing node transition rates, e.g. exhibiting nonlinearity and saturation effects that are highly relevant to social interactions.

We focus on social contagions where behaviors can be ‘healthy’ (positive) or ‘unhealthy’ (negative or infected) that are undesired. The foundation of the gLRIE strategy is its *minimum-risk-maximum-gain* principle promoting the positive against the negative diffusion in the context of competitive scenarios with conflicting node states (i.e. mutually exclusive). The strategy targets key individuals who pose the greatest transmission risk and, upon recovery, would exhibit a low probability of reinfection while simultaneously amplifying positive diffusion. gLRIE encompasses the LRIE strategy, and as such it constitutes a greedy but more refined way for reducing the number of *infectious edges*, i.e. edges connecting an infected and a healthy node and could channel the infection in the network.

Through rigorous theoretical analysis and extensive simulations on both synthetic and real-world networks, we demonstrate that positive diffusion serves as a potent counter-contagion force, significantly mitigating the complexity of the control problem. While this phenomenon is recognized in behavioral studies and health policy [28], [42], [43], yet its potential remains largely unexploited within the computational literature. Few studies have addressed the dynamic control of competing diffusion. Specifically, existing social contagion applications are limited to targeting problematic individuals, critically overlooking the capacity of pos-

itive diffusion to serve as a effect enhancer against contagion. This work bridges this gap by providing the theoretical and algorithmic framework necessary to operationalize this counter-force.

Finally, we move closer to a realistic counter-contagion campaign through a carefully designed use-case aiming to limit the spread of vaping among adolescents. Our simulated results suggest that intervention strategies can bring valuable gains against social contagion. The discussed control setting requires the administrator to be well-informed about the state of the network nodes, and to be also capable of intervening locally at the node-level. Although those requirements would need to get relaxed for large-scale applications, yet they may not be prohibitive in small well-monitored social environments, such as schools [28], [42], [43], penitentiary institutions [44], [45], working environments [46], nursing homes [47], [48], etc.

**Organization.** In the rest, Sec. 2 overviews the literature on competitive SIS models, coupled with a discussion on real-life case studies of behavioral epidemics to which our method is relevant. Sec. 3 focuses on the problem formalization and introduces the set of notations necessary for presenting the gLRIE algorithm in Sec. 4. Next, Sec. 5 outlines the experimental protocol and comparative simulations with competitive strategies, including a use-case on reducing vaping in a high school environment. Finally, Sec. 6 concludes this study and gives perspectives for future work.

## 2 MOTIVATION AND RELATED LITERATURE

In this section, we motivate both the direction of our technical contributions regarding modeling epidemics as well as the impact of resource allocation in real-world use-cases of social contagion.

### 2.1 Modelling competitive epidemics and control interventions

Coevolving epidemics offer a rich subclass of spreading processes where two or more virus strains try to take on the entire network, possibly one against the others. This setting has been mainly studied through extensions of the general SIS setting [24], and has then generated a lot of interest in the literature. In comparison, it is only recently that few studies appeared investigating competition for non-recurrent epidemic processes, namely under variations of the Susceptible-Infected-Removed (SIR) model [57], [64], [65]. Regarding the model of our interest, SIS, an indicative (but far from exhaustive) taxonomy of the main multi-virus SIS extensions is illustrated in Fig. 1, outlining results on the dynamics of spreading processes and their respective outcomes. A general epidemic setting is introduced in [51], where two viruses are spreading while interacting, and a parameter  $\epsilon$  defines either a competing ( $\epsilon < 1$ ) or a cooperating ( $\epsilon > 1$ ) nature for the process. A dynamical and linear algebra analysis allowed the determination of the different regimes of existence of one or both viruses in the steady-state. For cooperating epidemics, the spread of two co-infecting strains with a phase transition problem is formulated in [49] and [50]. Mutually exclusive epidemics have also been investigated in a variety of settings. Notably, in the scenario where two viruses spread within a single-layer network, a *winner takes all* phenomenon has been revealed where the virus with higher infectivity not only dominates, but even eradicates the other one [1]. The case of a bi-layer setting, i.e. two viruses spreading linearly over different contact networks involving the same set of nodes, is explored in [55] and [54]; the existence of steady-states of the epidemic where

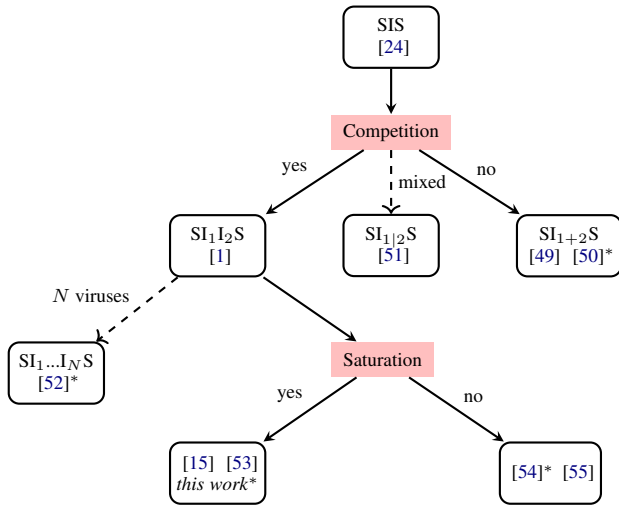


Fig. 1. **Overview of multi-virus SIS models.** Tree view of the main SIS extensions that consider multiple competing/cooperating infections spreading in a network. \* indicates articles that propose epidemic control strategies.

Spreading process	gLRIE features			
	Saturation	Diffusive healthy state	Control	Network data
Virus spread	[56] [53]	[53] [57]	[56] [53]* [57]* [6]* [58]*	[6] [58]
Crime, violence	[23] [22] [45]	[22]	[23] [45]	[22]
Positive / Negative sentiment	[42]	[15] [42] [46] [35] [59]	[35]*	[42] [59]
Obesity	[14] [43] [60]	[14] [16] [43] [60]	[14] [43] [60]	[43]
Tobacco use	[18] [61]	[18] [28] [17] [62] [63]	[18] [62] [61]* [28]	[28] [17] [62] [63]

TABLE 1

A selection of prior work on real-world epidemic and social contagion use-cases that are relevant to this study. References highlighted with lightgray correspond to analytic compartmental models, while gray ones correspond to agent-based models. The rest are data-driven studies. \* indicates articles proposing dynamic control strategies.

both viruses remain present is proven. This problem is generalized to an arbitrary number of linear spreading processes,  $SI_1 \dots I_N S$ , as well as for time-varying network structures [52].

Extensive research has been carried out on processes with a linear spread, although it has been observed that this assumption often overestimates the dynamics of the epidemic [42], [66], since they disregard the saturating infectivity. In fact, this type of propagation nonlinearity is the most relevant for social contagion. Regarding this issue, the work in [53] introduces a competitive SIS model with generic infection rates.

The aforementioned works provide comprehensive analytical insights into the progression of competitive epidemic processes, encompassing both general and advanced perspectives. These results can subsequently be employed in real-life case studies, which is what is discussed in the rest of this section.

## 2.2 Applications and use-cases

ABMs have been employed for modeling health-related behaviors [67], [68] and network intervention studies [69]. Tab. 1 provides an overview of several diverse application case-studies that have been investigated in the literature. The columns highlight the features that directly relate with this work, namely nonlinear saturating epidemic processes where two states are in competition, and for which control interventions can be applied to a known network.

In an epidemiological context, the spread of a disease within a population is approached by a variety of state-based models, each characterizing various compartments such as Susceptible, Exposed, Infected, Quarantined, Recovered, Removed/Dead, etc. The combination of these compartments depends on the properties of the epidemic, such as its time scale, the level of granularity, and other particular circumstances of the outbreak. Among the existing models, SIS constitutes the foundation for recurrent epidemics.

A direct application concerns interacting diseases, suggesting natural methods for disease control; for example, reducing Dengue transmission by introducing Wolbachia-infected mosquitoes [70], [71]. Computational models have been used to analyze the spread and of these two diseases in [72]. Additionally, dynamic resource allocation strategies are proposed to tackle problems such as limiting the propagation of diseases in livestock [58], or examining the infection spread within contact networks between patients and healthcare workers [6].

In a different context, several works have investigated social contagion phenomena related to public health issues, under the scope of competitive spreading processes. First, the sociology of delinquency in adolescence is investigated in [22] through school networks, while [23] introduces an ABM to encompass the dynamics of organized crime affiliation, with various intervention techniques. Next, the propagation of positive and negative emotions is tackled by a series of articles: for the Framingham Heart Study dataset [15], for the spread of mental health disorders through business networks [46], and for adolescent depression in high schools [42]. Obesity has been also a core subject of interest: e.g. in the case of adolescents with an ABM [43], or in generic networks via statistical analysis [14], [16], [60]. Similarly, the spread of tobacco use is investigated by quantitative studies [17], [28], [63] and compartmental epidemic models [18], [61], where the dynamics of the spreading process is studied along with optimal control strategies.

Several real-world pilot studies with deployed intervention experiments have been conducted in high schools. This specific setting is convenient for two reasons: a high school network forms a small ‘closed’ environment, in which the effect of peer influence is particularly important [73], [74]. Indeed, the repeated interaction between individuals is more frequent and intense than in other social contexts. Similarly, environments such as penitentiary institutions [45], working environments [46] and nursing homes [47] are also settings where social influence plays a key role in shaping behaviors, and this is the reason why they have been also the subject of various awareness-raising campaigns in the last decades in institutions [28], [44], [48].

Distinguishing true social influence from environmental factors and homophily remain significant challenges, particularly as network structures evolve alongside behaviors such as delinquency [22] or tobacco use [63]. Another important property of the set of applications listed above is that several real-world pilot studies with deployed intervention experiments focus on small ‘closed’

and well-monitored networks, e.g. high schools, nursing homes [47], and correctional facilities [45]. Unlike open networks, these environments feature high-intensity peer interactions [73], [74], creating strong amplification effects in diffusion processes. The application of the proposed framework to these specific settings represents an advancement beyond standard computational approaches and constitutes a step towards public-health intervention campaigns [28], [48]. Specifically, we provide a quantitative evaluation of how network-aware strategies can exploit this structural intensity to maximize positive behavioral change.

### 3 PROBLEM FORMULATION

#### 3.1 Setup and agent-based diffusion model

**Notations.** A graph  $\mathcal{G} = (\mathcal{V}, \mathcal{E})$  is a set of nodes  $\mathcal{V}$  representing the individuals in a population, let  $N = |\mathcal{V}|$ , which is also endowed with a set of edges  $\mathcal{E} \subset \mathcal{V} \times \mathcal{V}$ . It can be intuitively represented by its *weighted adjacency matrix*  $A \in \mathbb{R}_+^{N \times N}$ , where the element  $A_{ij} > 0$  if  $(i, j) \in \mathcal{E}$ , and  $A_{ij} = 0$  otherwise. We refer to directed graphs without self-loops, i.e.  $A_{ii} = 0, \forall i = 1, \dots, N$ . The *neighborhood* of node  $i$  is the set comprising all nodes connected to it with a directed edge, and is denoted by  $\mathcal{N}_i = \{i_k, \forall k \in \{1, \dots, d_i\} : (i_k, i) \in \mathcal{E}\}$ , where the node degree is  $d_i = \sum_j A_{ji}$ . Finally,  $\mathbb{1}\{\cdot\}$  is the indicator function.

**Continuous-time SIS subject to control via node treatments.** The  $N$ -intertwined continuous-time homogeneous SIS model [24], [75] describes the spread of a disease at each node of a graph. Each node (individual)  $i$  can be in either the *susceptible* or the *infected* state:  $X_i(t) = 0$  or  $1$ , respectively. The system at time  $t$  is globally characterized by the node state vector  $X(t) \in \{0, 1\}^N$ . Adopting the epidemic control aspect from [34], [76], with the addition of spontaneous infections, makes the state of node  $i$  evolve with the stochastic transition rates:

$$X_i(t) : \begin{cases} 0 \rightarrow 1 & \text{with rate } \alpha + \beta \sum_j A_{ji} X_j(t); \\ 1 \rightarrow 0 & \text{with rate } \delta + \rho R_i(t), \end{cases} \quad (3.1)$$

where  $\alpha$  is the rate of spontaneous node infections,  $\beta$  is the infection aggressiveness, and  $\delta$  is the self-healing capacity of a node. The epidemic control is realized by the resource allocation vector  $R(t) \in \{0, 1\}^N$ , whose coordinate  $R_i(t) = 1$  if we treat node  $i$  at time  $t$ , and  $0$  otherwise. Finally,  $\rho$  is the increase in recovery rate when a node receives a treatment resource. The model is homogeneous as all parameters are the same for all nodes ( $\alpha, \delta, \rho$ ) or edges ( $\beta$ ); this simplifies the presentation without being a modeling limitation. Moreover,  $\alpha$  and  $\delta$  can be considered as exogenous factors in the sense that they incur node state changes that are not due to the interactions within the network. Modeling bothwise spontaneous changes is particularly relevant in the context of social epidemics, as each individual is subject to both a self-correcting and self-undermining tendencies.

**A generic two-state recurrent epidemic model.** In this work, we introduce the following generic epidemic model.

**Definition 1.** Let two node-specific memoryless functions: the infection rate function  $\mathcal{I}_i$  and the  $\mathcal{H}_i$  healing rate function. A generic two-state recurrent epidemic model is then defined by the transition rates for each node  $i$ :

$$X_i(t) : \begin{cases} 0 \rightarrow 1 & \text{with rate } \mathcal{I}_i(X(t)); \\ 1 \rightarrow 0 & \text{with rate } \mathcal{H}_i(X(t)) + \rho R_i(t), \end{cases} \quad (3.2)$$

which induces a Markovian Poisson process with rate:

$$\lambda_i(t) = \mathbb{1}\{X_i(t) = 0\} \mathcal{I}_i(X(t)) + \mathbb{1}\{X_i(t) = 1\} \mathcal{H}_i(X(t)).$$

Since the administrator wishes to reduce the infection which has negative effects, we also call  $\mathcal{I}_i$  and  $\mathcal{H}_i$  as *positive/negative diffusion functions*. Those depend on the current network state  $X(t)$  and implicitly on the network structure (this is omitted from our notation). In our context, it is natural to additionally assume that  $\mathcal{I}_i$  and  $\mathcal{H}_i$  are monotonous w.r.t.  $X(t)$ :  $\mathcal{I}_i$  increases with  $X(t)$  and  $\mathcal{H}_i$  increases with  $\bar{X}(t)$ .

This SIS variant inherits the control mechanism from Model 3.1, namely the allocation of resources having stochastic treatment effect on individual nodes. Although this is not in the scope of this work, we may note that Model 3.2 suggests that control could also be attempted through global or local tuning of the  $\mathcal{I}_i$  or/and  $\mathcal{H}_i$  function shapes.

#### 3.2 Dynamic resource allocation

Dynamic interventions are meaningful when the the time-scale needed for the interventions to take effect is comparable to the speed of the epidemic (i.e. node state transitions). In the *Dynamic Resource Allocation* (DRA) problem [34], [76], an SIS model variant (Model 3.1) is admitted, and the objective is to administer a budget of  $b$  treatment resources (units), each having strength  $\rho$ , in order to suppress an undesired state that diffuses. The treatments cannot be stored for later use ( $\sum_i R_i(t) \leq b, \forall t$ ), and their effect is limited as a node can receive at most one treatment ( $R_i(t) \in \{0, 1\}, \forall t, i$ ). Dynamic score-based strategies, which invoke the resource re-allocation procedure in Alg. 1 whenever intervention is possible, can provide efficient solutions to the DRA problem and are rather simple to implement. A greedy dynamic score-based strategy is developed in [34], called *Largest Reduction in Infectious Edges* (LRIE). Each node is assigned a score that quantifies its criticality for the future spread of the infection.

Other score-based solutions have been proposed, e.g. based on fixed Priority Planning [76], or static ones based on spectral analysis [30], [31] (see details in Sec. 5). In a complementary research direction, such scoring functions have also been used in Restricted- and Sequential-DRA settings [7], which constrain the administrator so she can access and intervene only to few nodes through resource allocation.

### 4 GENERALIZED LARGEST REDUCTION IN INFECTIOUS EDGES: ANALYSIS AND ALGORITHM

We propose the DRA strategy named *Generalized Largest Reduction in Infectious Edges* (gLRIE) that at each time identifies and treats in a greedy fashion the most critical nodes in order to reduce the epidemic as quickly as possible. The gravity of the epidemic can be expressed in terms of the number of infected nodes at time  $t$ , denoted by  $N_I(t) = \sum_i X_i(t)$ . The approach generalizes the LRIE strategy [34] to a broader class of epidemics, featuring also competition, which is the main interest of this work. In a Markovian setting, given the fixed characteristics denoted by  $\Lambda$  (i.e. the graph structure and the characteristics of the propagation), and the instantaneous state of the population  $X(t)$ , the best intervention expressed by the resource allocation vector  $R$  in Model 3.1 and Model 3.2 that would minimize the cost function:

$$C(\Lambda, X, \gamma) = \int_{u=0}^{\infty} e^{-\gamma u} \mathbb{E}[N_I(t+u) | X(t) = X] du. \quad (4.1)$$

**Algorithm 1** Generic score-based DRA control strategy\*

**Input** : adjacency matrix  $A$ ; network state  $X(t)$  at time  $t$ ; budget available  $b$

**Output** : resource allocation vector  $R(t)$ , with 1 for targeted nodes and 0 otherwise, while respecting the budget  $\sum_{i=1}^N R_i(t) \leq b$

---

```

1: for  $i = 1, \dots, N$  do
2:    $S_i \leftarrow \text{computeScore}(i, X(t), A)$ 
3: end for
4:  $\text{nodeRanking} \leftarrow \text{sort}(S)$ 
5:  $R(t) \leftarrow \text{selectTop}(\text{nodeRanking}, \min(b, \sum_i X_i(t)))$ 
6: return  $R(t)$ 
    
```

---

\* Resource re-allocation occurs each time the control strategy gets invoked for intervening to the spreading process, and the resources remain in effect on the target nodes until a next update.

$\Lambda$  remains fixed throughout the process, so we omit it from the rest of the notations. The cost function is parametrized by  $\gamma \in \mathbb{R}_+$  that can be chosen so as to give emphasis on short-term effects. Considering  $\Phi_{t,X}(u) = \mathbb{E}[N_I(t+u) | X(t) = X]$  and then taking the Taylor series expansion w.r.t.  $u$  at 0, yields:

$$(4.1) \quad \frac{1}{\gamma} \Phi_{t,X}(0) + \frac{1}{\gamma^2} \Phi'_{t,X}(0) + \frac{1}{\gamma^3} \Phi''_{t,X}(0) + \mathcal{O}\left(\frac{1}{\gamma^4}\right). \quad (4.2)$$

Next, we present the final results of the derivation of each of the three first terms, while their detailed evaluation can be found in Appendix A. As treatments are always administered to infected individuals, let us concentrate at an infected node  $i$ . At this point, it is convenient to define the generic rate function  $\mathcal{F} \in \{\mathcal{H}, \mathcal{I}\}$  to refer to both the positive or the negative diffusion, and special notations for the updates on  $\mathcal{F}_j$ ,  $j \neq i$ , in the hypothetical case where node  $i$  recovers, and that recovery to be the only change occurred in the network:

$$\begin{aligned} \mathcal{F}_j^{-i} &= \mathcal{F}_j(X_1, \dots, X_i = 0, \dots, X_N), \\ \Delta \mathcal{F}_j^{-i} &= \mathcal{F}_j - \mathcal{F}_j^{-i}. \end{aligned} \quad (4.3)$$

In this sense, Eq. 4.3 produces the four definitions:  $\forall j \neq i$ ,  $\mathcal{H}_j^{-i}$ ,  $\mathcal{I}_j^{-i}$ ,  $\Delta \mathcal{H}_j^{-i} = \mathcal{H}_j - \mathcal{H}_j^{-i} \leq 0$ , and  $\Delta \mathcal{I}_j^{-i} = \mathcal{I}_j - \mathcal{I}_j^{-i} \geq 0$ . The last two give the difference in the rates after a hypothetical recovery of node  $i$ . Their signs are so due to  $\mathcal{H}_i$  (resp.  $\mathcal{I}_i$ ) being monotonically decreasing (resp. increasing) with the infection level  $X(t)$ , and the fact that any node recovery essentially reduces  $X(t)$ . Therefore, the final forms of the derivatives appearing in Eq. 4.2 become:

$$\Phi_{t,X}(0) = \sum_i X_i, \quad (4.4)$$

$$\Phi'_{t,X}(0) = - \sum_i \mathcal{H}_i X_i - \rho \sum_i R_i X_i + \sum_i \mathcal{I}_i \bar{X}_i, \quad (4.5)$$

$$\begin{aligned} \Phi''_{t,X}(0) &= \Xi(t) + \rho \sum_i X_i R_i \left\{ (\mathcal{H}_i + \mathcal{I}_i) + \right. \\ &\quad \left. + \sum_{j \neq i} \left[ X_j (\Delta \mathcal{H}_j^{-i}) - \bar{X}_j (\Delta \mathcal{I}_j^{-i}) \right] \right\}, \end{aligned} \quad (4.6)$$

where we let  $\bar{X}_i = 1 - X_i$ , and  $\Xi(t)$  to be a function that absorbs any terms that are independent to  $R_i$ . The terms of the expansion describe the effects of healing a node (i.e. after it recovers) on the network. The first two trivially suggest treating only infected nodes. The third one (second order term), though, quantifies the contribution of managing to heal a specific node to

the minimization of the cost function. According to Eq. 4.6, we derive the following gLRIE score for each infected node  $i$ :

$$S_i = - \left[ \underbrace{(\mathcal{H}_i + \mathcal{I}_i)}_{\substack{\text{effect on } i \\ \text{self-healing and} \\ \text{social healing}}} + \underbrace{\sum_{j \neq i} \left[ X_j (\Delta \mathcal{H}_j^{-i}) - \bar{X}_j (\Delta \mathcal{I}_j^{-i}) \right]}_{\substack{\text{effect of the supposed healed } i \text{ on the network} \\ \text{vulnerability} \quad \text{contribution to} \\ \text{social healing} \quad \text{virality}}} \right]. \quad (4.7)$$

**Interpretation.** To discuss the rationale of the score in Eq. 4.7, we distinguish two parts. The first is the quantification of node  $i$ 's total transition rate,  $\mathcal{H}_i + \mathcal{I}_i$ : this says that if  $i$  could get easily reinfected (high  $\mathcal{I}_i$ ) or/and could anyway recover rapidly due to self-healing and positive diffusion that we call ‘‘social healing’’ (high  $\mathcal{H}_i$ ), then it is not a good candidate to invest resources on. The second part quantifies the effect that a supposed recovered  $i$  would bring to the network: by recalling that always  $\Delta \mathcal{H}_j^{-i} \leq 0$  and  $\Delta \mathcal{I}_j^{-i} \geq 0$ , we can see that gLRIE assigns higher scores to prioritize nodes that would bring a high gain in social healing (high negative  $\Delta \mathcal{H}_j^{-i}$  value for infected  $j$ ) and a big drop of infectivity (high positive  $\Delta \mathcal{I}_j^{-i}$  value for healthy  $j$ ). Fig. 2 illustrates how the various factors related to the positive and the negative diffusion are taken into account when computing the gLRIE scores.

Notice that the locality of the gLRIE score is determined by the definition of the functions  $\mathcal{H}_i$  and  $\mathcal{I}_i$ , and can potentially depend on the whole network. In the next section, we introduce assumptions to arrive to a variant of this score that is simpler and more useful in practice.

#### 4.1 Simplified gLRIE score

The score-based strategy suggested by Eq. 4.7 can be simplified under three rather standard assumptions in SIS modeling, concisely expressed in terms of the generic rate function  $\mathcal{F} \in \{\mathcal{H}, \mathcal{I}\}$  (see Eq. 4.3).

- **Assumption 1 – Locality:** The transition rate of each node  $i \in \mathcal{V}$  depends only on its neighbors  $i_1, \dots, i_{d_i} \in \mathcal{N}_i$ :

$$\mathcal{F}_i = \mathcal{F}_i(X_{i_1}, \dots, X_{i_{d_i}}). \quad (4.8)$$

- **Assumption 2 – Exchangeability:** The transition rate of each node  $i \in \mathcal{V}$  is invariant to the node permutations ( $\pi$ ) of its neighbors:

$$\mathcal{F}_i(X_{i_1}, \dots, X_{i_{d_i}}) = \mathcal{F}_i(X_{\pi(i_1)}, \dots, X_{\pi(i_{d_i})}). \quad (4.9)$$

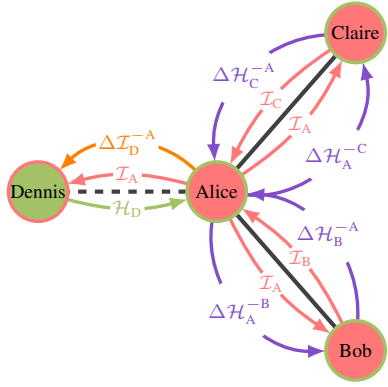
- **Assumption 3 – Homogeneity:** The transition rate functions are the same for all nodes  $i \in \mathcal{V}$ :

$$\mathcal{F}_i = \mathcal{F}, \quad \forall i \in \{1, \dots, N\}. \quad (4.10)$$

Assumptions 1-2 restrict the class of rate functions to those that only depend on a node's neighborhood state and size. Indeed, given the node degree  $d_i$ , the state of its neighborhood  $\{X_{i_1}, \dots, X_{i_{d_i}}\} \in \{0, 1\}^{d_i}$ , and the number of infected neighbors  $n_i = \sum_j A_{ji} X_j$ , we have for all  $i \in \mathcal{V}$ :

$$\mathcal{F}_i(X_1, \dots, X_{d_i}) = \mathcal{F}_i(\overbrace{1, \dots, 1}^{n_i}, \overbrace{0, \dots, 0}^{d_i - n_i}) =: \mathcal{F}_i(n_i, d_i). \quad (4.11)$$

Due to Assumption 1, for any node  $j$  non-adjacent to  $i$ , it holds  $\forall j \notin \mathcal{N}_i: \Delta \mathcal{F}_j^{-i} = \Delta \mathcal{F}_i^{-j} = 0$ . Moreover, as Assumption 2



(a) Contact network (straight black edges) and factors affecting node scores (colored arcs).

Node $i$	$\mathcal{H}_i$	$\mathcal{I}_i$	$\sum_j \Delta \mathcal{H}_j^{-i}$	$\sum_j \Delta \mathcal{I}_j^{-i}$	$S_i^{\text{gLRIE}}$	$S_i^{\text{LRIE}}$
Alice	$\delta$	$2\beta$	$-2\gamma$	$\beta$	$-\delta - \beta + 2\gamma$	$-\delta - \beta$
Bob	$\delta$	$\beta$	$-\gamma$	$0$	$-\delta - \beta + \gamma$	$-\delta - \beta$
Claire	$\delta$	$\beta$	$-\gamma$	$0$	$-\delta - \beta + \gamma$	$-\delta - \beta$
Dennis	$-$	$-$	$-$	$-$	$-$	$-$

(b) The factor values used to compute the gLRIE and LRIE scores.

**Fig. 2. Minimal example comparing gLRIE and LRIE scores.** a) A simple undirected and unweighted contact network between 4 individuals, 3 of which are infected. The edges between agents are shown as straight black lines, out of which those being dashed are the *infectious edges* that connect nodes in different states and hence can channel both positive and negative diffusion. The factors involved in gLRIE score (Eq. 4.7) appear as labeled arcs. Node boundaries, green for infected and red for healthy nodes, indicate the spontaneous self-healing and self-infection, respectively. b) Table with the values of the factors involved in the gLRIE and LRIE scores for an infected node  $i$ , in the case of linear infection. The parameters  $\delta$ ,  $\gamma$ , and  $\beta$  are the self-healing, social healing, and social infection rates, respectively. The gLRIE score prioritizes Alice over Bob and Claire, due to the added contribution of social healing she could bring when she would have recovered, while LRIE treats them equally. Dennis being healthy, he is not considered for receiving a treatment.

renders neighbors indistinguishable, we can eliminate the reference to node  $i$  from the notations in Eq. 4.3:  $\forall i \in \mathcal{N}_j : \mathcal{F}_j^- \equiv \mathcal{F}_j^{-i}$  and  $\Delta \mathcal{F}_j^- \equiv \Delta \mathcal{F}_j^{-i}$ . Let us bringing the explicit  $\mathcal{H}_i$  and  $\mathcal{I}_i$  back in the discussion. According to Assumption 3, we can consider that the same positive and negative transition rate functions act on all the network nodes, which writes:

$$\begin{aligned} \mathcal{I} &= \mathcal{I}(n_i, d_i), \\ \mathcal{H} &= \mathcal{H}(n_i, d_i). \end{aligned} \quad (4.12)$$

The above assumptions and discussion lead to Remarks 1-3.

**Remark 1. Encompassing the standard SIS model.** Given Assumptions 1-3, the standard SIS Model 3.1 can be recovered by the introduced Model 4.12 by setting:

$$\begin{aligned} \mathcal{I}(n_i, d_i) &= \beta \sum_j A_{ji} X_j = \beta n_i, \\ \mathcal{H}(n_i, d_i) &= \delta. \end{aligned} \quad (4.13)$$

**Remark 2. Simplified gLRIE score.** Assumptions 1-3 yield the following simplified variant of the gLRIE score:

$$S_i = - \left[ (\mathcal{H}_i + \mathcal{I}_i) + \sum_j A_{ij} \left[ X_j (\Delta \mathcal{H}_j^-) - \bar{X}_j (\Delta \mathcal{I}_j^-) \right] \right]. \quad (4.14)$$

Compared to the more generic Eq. 4.7, this score is local as the transition functions and the summation look only at the neighborhood of node  $i$  (recall also that the adjacency matrix  $A$  has a zero diagonal).

**Remark 3. Equivalence of gLRIE and LRIE score rankings.** Under the standard SIS Model 3.1 without competition, the scoring function gets a form as in Remark 1, with:

$$\begin{aligned} \mathcal{I}_i &= \alpha + \beta \sum_j A_{ji} X_j, \\ \mathcal{H}(n_i, d_i) &= \delta, \\ \Delta \mathcal{H}_j^- &= 0, \\ \Delta \mathcal{I}_j^- &= \beta. \end{aligned} \quad (4.15)$$

Then, the simplified gLRIE score (Eq. 4.14) reduces to:

$$S_i = - \left[ (\alpha + \delta) + \beta \sum_j A_{ji} X_j - \beta \sum_j A_{ij} \bar{X}_j \right], \quad (4.16)$$

which is equivalent to the LRIE score up to the constant term  $\alpha + \delta$  that does not affect node ranking.

**Algorithm and computational complexity.** At time  $t$ , the gLRIE strategy takes as input the network state  $X(t)$  and the budget of resources  $b$ ; it computes independently the criticality score for each node (Eq. 4.7); ranks the nodes according to their scores; finally, it treats as many nodes as the budget allows, i.e.  $\sum_i R(t) = \min(b, \sum_i X_i(t))$ . The simplified gLRIE scoring function (Eq. 4.14) reduces the computational complexity of the strategy (Alg. 1) to  $\mathcal{O}(Nd_{\max} + N \log N)$ , where  $d_{\max}$  is the maximum node degree.

**Discussion.** The main contribution of this paper is the generic gLRIE scoring strategy that relies on a SIS model reformulation, and is suitable for multiple recurrent spreading processes in a network. gLRIE bears a number of properties, some of which are inherited by the DRA formulation and its greedy approach, and therefore are shared with the included LRIE, while others stem from the introduction of the generic positive and negative diffusion functions:

- **Generic transition rates:** To capture the complexity of social interactions, both the positive and negative diffusion rates are designed to be generic, exhibiting saturating effects and exogenous intensity to assimilate social influence outside the network, and can potentially vary for each individual.
- **Distributivity:** As a strategy relying on local scores, gLRIE allows independent score computations at individual nodes, and requires only a centralized score ranking.
- **Adaptivity:** It exhibits adaptability to changes of the network structure, which is relevant in scenarios involving dynamic networks emerging in behavioral epidemics, or in controversial

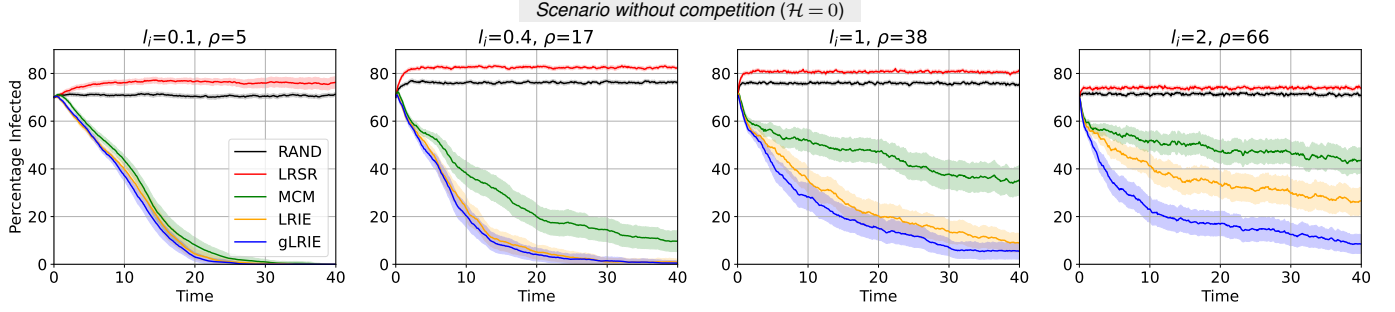


Fig. 3. **Evolution of a single epidemic from linear to nonlinear spreading for different intervention strategies.** The percentage of infected nodes over time in Erdős-Rényi graphs of 300 nodes with average degree 8, when different strategies are employed. *Only the negative diffusion is considered* ( $\mathcal{H} = 0$ ). Each plot shows an average over 1000 simulations of the generalized SIS Model 3.2 using Eq. 5.1. From (a) to (d), the diffusion moves from being essentially linear to nonlinear. The saturation level is fixed to  $s_{\mathcal{T}} = 10$ , and the number of resources to allocate is  $b = 10$ .

public debates that frequently trigger dramatic changes in the contact network in short time.

- *Edge directionality*: Taking into account edge directionality is essential in the context of social contagion. This is taken into account to ensure comprehensive coverage.

## 5 SIMULATIONS

In this section, we first present our experimental setup, the specific diffusion functions we choose for gLRIE, the competitors we choose from the literature. Next, we present simulations on random and real networks that validate the core properties of gLRIE. Finally, we design a semi-synthetic experiment that illustrates the applicability of our approach to real-world campaigns.

### 5.1 Experimental setup

**Diffusion functions.** We employ the generalized SIS Model 3.2. In order to encompass particular aspects in social behaviors, such as *nonlinearity* and *saturation* in the node transition rates, we consider sigmoid functions:

$$\begin{aligned} \mathcal{I}(n, d) &= \alpha + s_{\mathcal{T}} \left[ 1 - \frac{2}{1 + \exp\left(2\ell_{\mathcal{T}} \frac{n}{\xi}\right)} \right]; \\ \mathcal{H}(n, d) &= \delta + s_{\mathcal{H}} \left[ 1 - \frac{2}{1 + \exp\left(2\ell_{\mathcal{H}} \frac{(d-n)}{\xi}\right)} \right], \end{aligned} \quad (5.1)$$

where  $s_{\mathcal{T}}$  (resp.  $s_{\mathcal{H}}$ ) parameter controls the saturation level and  $\ell_{\mathcal{T}}$  (resp.  $\ell_{\mathcal{H}}$ ) the slope at the origin. Recall that  $n$  is the number of infected neighbors,  $d$  is the node degree, while  $\xi \in \{1, d\}$  is a normalization term that makes the state transition rate of a node dependent to either the number ( $\xi = 1$ ) or the fraction ( $\xi = d$ ) of its neighbors being in the opposing state. Without loss of generality, we henceforth set  $\xi = 1$  that takes explicitly into consideration the fact that individuals' limited total capacity may allow social interaction with a small number of their contacts each time. The above equations are expressed for the case of an unweighted and undirected graph. For a directed graph without weights,  $d$  would be replaced by the node in-degree  $d_{\text{in}}$ . For a weighted graph,  $n$  could be replaced by the weighted sum of infected neighbors ( $\sum_j A_{ji} X_j$ ), and  $d$  by the weighted sum of all neighbors ( $\sum_j A_{ji}$ ). The functions  $\mathcal{I}$  and  $\mathcal{H}$  are repetitively evaluated on a finite and discrete set of points,  $(n, d) \in \{0, 1, \dots, d_{\text{max}}\}^2$ , therefore, they could be precomputed in two matrices of size

$(d_{\text{max}} + 1) \times (d_{\text{max}} + 1)$  each, and retrieved in constant time during simulations.

**Other strategies.** As a naive baseline, we use the Random Allocation (RAND) that targets infected nodes at random. The second competitor is the Largest Reduction in Spectral Radius (LRSR) [30], which is based on spectral graph analysis generalized to arbitrary healing effects ( $\rho \neq \infty$ ). LRSR selects nodes that maximize the eigen-drop of the largest eigenvalue of the adjacency matrix, known as *spectral radius*. Next comes the MaxCut Minimization (MCM) [76], which uses the *priority planning* approach. The strategy proceeds according to a precomputed node *priority-order* that is a linear arrangement of the network with minimal *maxcut*, i.e. maximum number of edges need to be cut in order to split the ordering in two parts.<sup>1</sup> The last most direct competitor is the greedy dynamic LRIE strategy [34] that is generalized in this work.

**Evaluation metrics.** There are various metrics for evaluating the quality of a strategy, e.g. expected extinction time, final percentage of infection, area under the curve (AUC). We choose as main measure the AUC as it provides useful measurements even if a strategy does not remove completely the infection, which is a limitation of the expected extinction time. AUC accounts for the total number of infected nodes throughout time, which, in a socioeconomic context, is more interesting than the final infection size. Further, by fixing using the diffusion parametrization  $\{s_{\mathcal{T}}, \ell_{\mathcal{T}}, s_{\mathcal{H}}, \ell_{\mathcal{H}}\}$ , we compare gLRIE to a competitor by:

$$\text{AUC-ratio} = \frac{\text{AUC}(\text{gLRIE})}{\text{AUC}(\text{Competitor})}. \quad (5.2)$$

### 5.2 Random Networks

In this section, we present comparative experiments in random networks. First we introduce gradually nonlinearity and saturation in the diffusion, and then we also show the effects of competition. To this end, we use Erdős-Rényi (ER), Preferential Attachment (PA), and Hierarchical Erdős-Rényi (hierER) random networks of comprising 300 nodes each. The hierER networks have hierarchical community structure. First, isolated Erdős-Rényi clusters are created at the lowest level of the hierarchy. Then, a cluster at the  $l$ -th level is formed by combining a non-intersecting subset of clusters of the  $l-1$ -th level, by adding Erdős-Rényi inter-cluster connections that become weaker as  $l$  grows.

<sup>1</sup> The comparison with the CURE algorithm [33] is omitted, as in [76] it has been shown to have inferior and less stable performance compared to MCM.

Scenario without competition ( $\mathcal{H} = 0$ )    Scenario with competition ( $\mathcal{H} \neq 0$ )

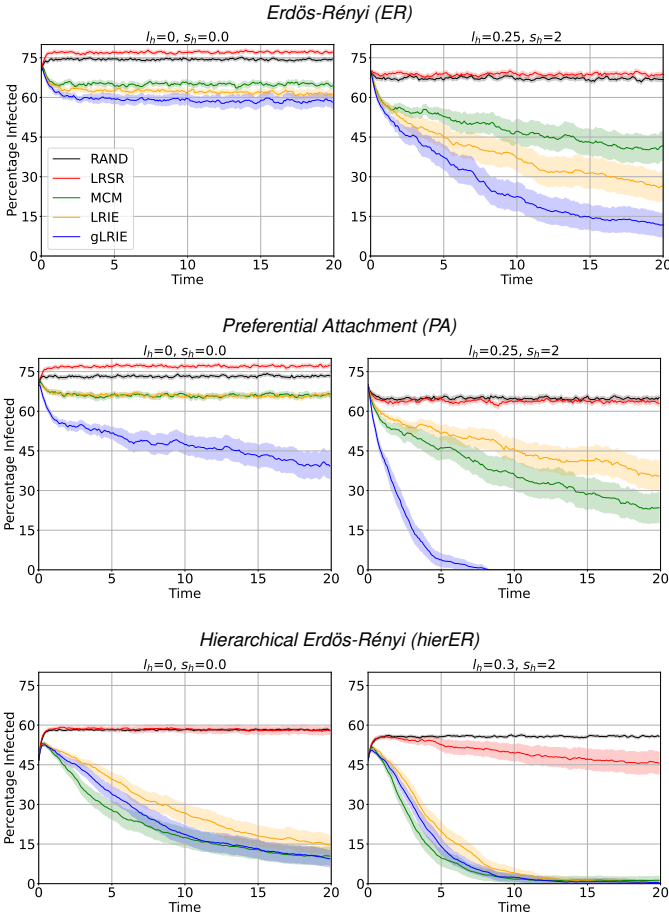


Fig. 4. **Evolution of nonlinear SIS processes with and without competition, under various intervention strategies.** Percentage of infected nodes under the generalized SIS Model 3.2 using Eq. 5.1, when different strategies are employed. Results for ER (a,b), PA (c,d), and hierER (e,f) networks, 300 nodes in each case. In the plots on the left, healthy states do not diffuse ( $\mathcal{H} = 0$ ). On the right though, there is competition between the positive and negative diffusion ( $\mathcal{H} \neq 0, \mathcal{I} \neq 0$ ). The model's parameters are set to:  $s_{\mathcal{I}} = 10, \ell_{\mathcal{I}} = 2$  for the negative diffusion, and  $s_{\mathcal{H}} = 2, \ell_{\mathcal{H}} = 0.25$  for the positive diffusion (when present). At any moment in time, up to  $b = 10$  nodes are targeted with resource units of  $\rho = 155$  healing strength.

**Introducing nonlinearity and saturation.** We first consider only the negative diffusion (i.e.  $\mathcal{H} = 0$ ) and we gradually increase  $\ell_{\mathcal{I}}$  in an ER random graph, moving gradually from linear (as in the standard SIS model) to nonlinear saturating functions. Fig. 3 shows the average over 1000 simulations of the percentage of infected nodes over time and the 95% confidence interval under the hypothesis of Gaussian distribution of the results. The results indicate that in the presence of a saturating infection rate, our strategy becomes much more efficient than the competitors. **Introducing competition.**

Fig. 4 presents the effects of positive diffusion that is embedded in the function  $\mathcal{H}$ , on ER, PR, and SW random networks. To observe more clearly the role of the strategies, we chose to have a less diffusive healthy state compared to the infected state. The simulations show that, unlike gLRIE, the methods of the literature lack modeling power to deal efficiently with this complex setting involving saturation as a result of nonlinearity and competition. On the other hand, gLRIE does not take into account high-level network structure, which is a strength of the MCM strategy (see the hierER example in Fig. 4).

### 5.3 Real Networks

We performed simulations on the *Polblogs* dataset [77], a directed network of 1222 nodes and 19090 edges representing hyperlinks between political blogs around the time of the 2004 US presidential election, as well as on the *Ugandan health advice* social network of Ugandan households exchanging health advice in villages [78], containing 361 nodes and 1360 edges. Two scenarios were considered, with and without positive diffusion, over a wide parameterization range that allows us to observe the capacity of a strategy to control an infection by affecting a minimal set of agents.

Fig. 5 summarizes the empirical results: the first row of heatmaps refers to the scenario with neutralized positive diffusion ( $\mathcal{H} = 0$ ), contrary to the second row. Each grayscale heatmap shows the final infection size when applying gLRIE; in the black regions the infection is completely removed, while the brighter part indicates persistence at the end of the simulation. Each colored heatmap, compares gLRIE to one of the competitors (LRIE and MCM) by showing a landscape of AUC-ratio values (Eq. 5.2) over a 2d parametrization. In each heatmap, the shape of the function  $\mathcal{H}$  of the positive diffusion is fixed, while the shape of the function  $\mathcal{I}$  of the negative diffusion varies: its saturation level increases ( $s_{\mathcal{I}}$ ) along the x-axis, and its slope ( $\ell_{\mathcal{I}}$ ) increases along the y-axis. For simplicity, we set for the exogenous rates  $\alpha, \delta = 0$ , as they merely cause a time shift to the diffusion outcome.

The color heatmaps highlight three regimes. On the top-left side of a heatmap, the diffusion parameters define a weak infection for which any strategy would perform well. Contrary, on the bottom-right side, the infection becomes harder to control for all strategies, with the given budget of resources. Moreover, in the left border, the low saturation level causes  $\mathcal{I}$  to already saturate with just one infected neighbor. When  $\mathcal{I}$  is almost linear and  $\mathcal{H} = 0$ , gLRIE and LRIE appear to be equivalent. Overall, those heatmaps exhibit a clear pattern with a right-curve-shaped darker area where gLRIE overpowers systematically all competitors, showing that it is the most versatile and best performing strategy in the considered competitive spreading setting.

### 5.4 Semi-synthetic high school anti-vaping campaign

The final experimental scenario simulates an intervention strategy aiming at reducing the number of vaping students in a monitored high school environment. In response to the emergence of applied intervention programmes to prevent nicotine use in the past two decades [17], [28], [79], research in developing effective strategies to prevent cigarette use have been developed [18], [61]. More recently, a growing body of literature on vaping among adolescents [62], [63], [80] has highlighted the need for effective intervention strategies to curb its spread, e.g. through counseling sessions or educational programs. Motivated by this problem, we design a series of intervention simulations based on real-world social network data to evaluate the performance of gLRIE and other strategies. It should be noted that some of the real campaigns target nodes regardless their state, aiming to increase the self-resistance of susceptible nodes and their positive influence to peers. This can be a future extension, however, we adapt the simulations as our current model targets infected nodes only.

**Calibration of the vaping experiment.** We use a publicly available adolescent network from a high school in Spain [81], which contains 409 nodes and 8557 directed edges representing static asymmetric influence relationships. This is a class of students

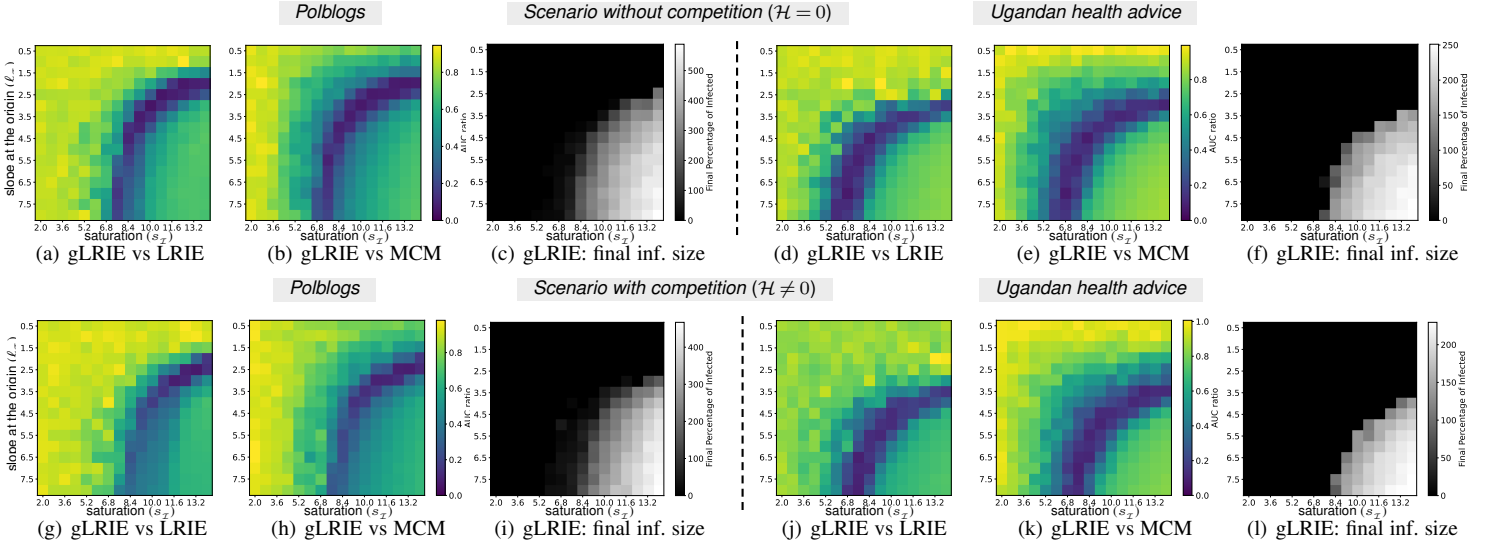


Fig. 5. **Pairwise performance comparison between the gLRIE, LRIE, and MCM intervention strategies via simulations on real datasets.** Left (resp. right) columns: heatmaps of the AUC-ratio between gLRIE and competitors, using the generalized SIS model (Eq. 5.1) in the Polblogs (resp. health-advice) network with  $b = 30$  and  $\rho = 130$  ( $b = 10$  and  $\rho = 80$ ). The first row corresponds to the scenario with no positive diffusion, while the second row is the case where positive diffusion is present. The color map ranges from yellow (ratio = 1), where the strategies perform the same, to blue (ratio = 0), where only gLRIE manages to remove the infection. As expected, the positive diffusion reduces the difficulty of the control problem.

considered as a small ‘closed’ community over a 3-year period, from the 10th to the 12th grade, during which the vaping behavior is monitored. To ensure realistic dynamics, we calibrate the diffusion model underlying gLRIE using data from the *Monitoring the Future* study [82]. This longitudinal survey reports that the percentage of vaping 10th grade students (with or without nicotine) is approximately 20%, which increases to 28% by the 12th grade in the absence of control. To simulate this background tendency in absence of control, we set the diffusion parameters to  $s_x = 8$ ,  $l_x = 2$ ,  $s_H = 8$ , and  $l_H = 0.5$ . The asymmetric diffusion intensity reflects the observation that vaping initiation tends to be more contagious than cessation in adolescent populations.

**Intervention protocol.** We evaluate the effectiveness of the intervention strategies as a function of three key operational parameters: treatment strength ( $\rho$ ) on an individual, budget ( $b$ ) that is the maximum number of students targeted simultaneously, and the intervention frequency ( $f$ ) corresponding to how often the set of targeted students is revised. To focus on intervention planning, we present results that vary  $b$  and  $f$ , keep fixed  $\rho = 40$ , and simulate over a period of 36 months, i.e. the 3-year high school duration. We explore different intervention plans:  $f = \{12 : \text{monthly}, 4 : \text{trimesterly}, 2 : \text{semesterly}, 1 : \text{annually}\}$ . We compare gLRIE with two simple and realistic baselines: the random nodes (RAND) and the highest out-degree nodes (HDN) among those being infected.

**Results.** Fig. 6 illustrates the temporal evolution of the percentage of vaping students under the different intervention strategies. Similarly to the heatmaps presented in Fig. 5, the cases at the top left side are easier to deal with, while those at the bottom right are harder. The results demonstrate that, although the difference is not substantial in every parametrization scenario, gLRIE is consistently the best strategy over the time period, followed by HDN and RAND. Notably, at high budget, a decrease of the vaping prevalence is visible for gLRIE but not for the other strategies. Next, we evaluate the relationship between the final percentage of vaping students and the overall campaign cost expressed as

$b \times f$ . In Fig. 7, lines represent different budget levels, with varying frequencies indicated by dot sizes. In addition to gLRIE’s superior performance, the results highlight that budget has greater contribution than frequency in reducing vaping prevalence. This suggests that coordinated interventions targeting more students at once are more effective than allocating resources thinly over time, whose effect tends to saturate faster. In the simulated time-frame, the absolute difference in infection percentage may seem moderate at a first glance. However, Fig. 8 shows the relative difference over time in infection size between HDN and gLRIE, when the effect of each of them is expressed relatively to the result of RAND. This allows to better appreciate the consistent advantage of gLRIE, which, in strong intervention scenarios, achieves more than 10% relative reduction in vaping prevalence compared to RAND, whereas HDN only reaches 5%. It can be observed that the effects of gLRIE (resp. HDN) start deviating at around 6 months (resp. 1 year) in the simulation for most scenarios, which suggests that early interventions may not yield immediate benefits, but their impact accumulates over time.

**Sensitivity and feasibility analysis – Impact.** It should be noted that gLRIE is the only method that requires information about both the network structure and the diffusion parameters, which may not always be available in practice. In contrast, HDN relies solely on network topology, making it more feasible to deploy in real-world applications. It is therefore natural to assess the performance gain of gLRIE in view of its requirement for additional information. To this end, we conduct a sensitivity analysis to assess the gLRIE’s robustness to inaccuracies (over- or under-estimation) in the used slope and saturation parameters involved in the infection and healing diffusion functions used in the gLRIE score computation. The results in Fig. 9, indicate that gLRIE maintains a significant performance advantage over HDN across different scenarios, even with substantial parameter misestimation.

This semi-synthetic use-case provides empirical evidence about the potential of considering intervention strategies that leverage both network information and positive diffusion, to optimize resource allocation in small-scale and well-monitored social

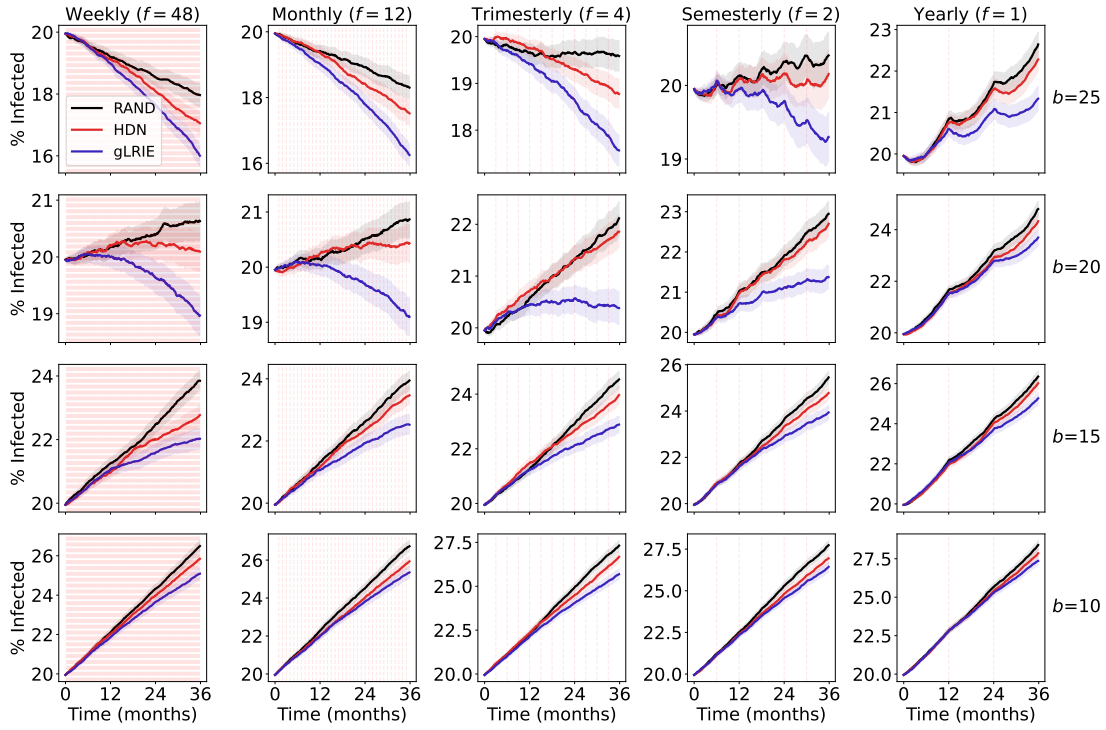


Fig. 6. Temporal evolution of the percentage of vaping students in a high school social network over a 3-year period. The generalized SIS model (Eq. 5.1) is used with  $s_I=8, l_I=1$  for the negative diffusion, and  $s_H=8, l_H=0.5$  for the positive diffusion. At each intervention time (dashed vertical line), up to  $b$  nodes are targeted with resource units of  $\rho = 40$  healing strength. Averaged results over 400 simulations are plotted.

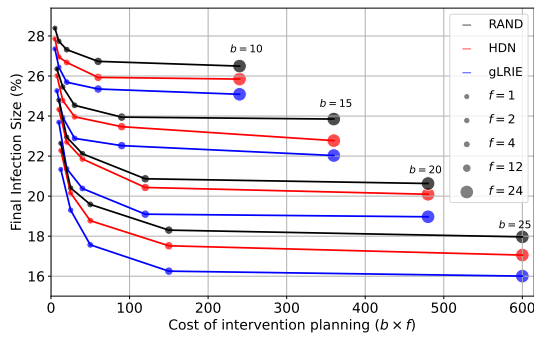


Fig. 7. Final percentage of vaping students, after a 3-year period, as a function of total treated students for the RAND, HDN and gLRIE strategies. Each line corresponds to a different intervention budget ( $b$ ) with varying intervention frequency ( $f$ ), represented by dot sizes.

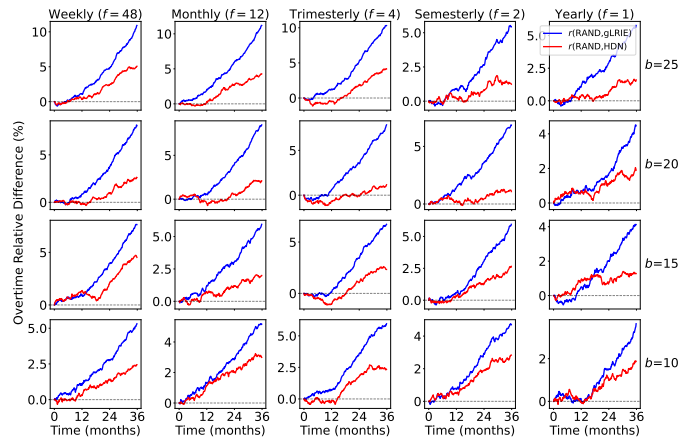


Fig. 8. Evolution of the relative difference in infection size between the HDN and gLRIE strategies. The effect of each of the compared strategies is expressed relatively to the result of the RAND baseline. The results correspond to the same intervention scenarios as in Fig. 6. Averaged results over 400 simulations are plotted. Higher positive values imply larger gains compared to RAND.

environments, such as public health campaigns within school settings, penitentiary or healthcare institutions. Notably, distinct effects are observed: increasing the budget ( $b$ ) leads to a more pronounced reduction in vaping prevalence, as more students can be targeted simultaneously. Conversely, increasing the intervention frequency ( $f$ ) results in a more temporally smooth and sustained effect over time, but of rather smaller effect in reducing the magnitude of the contagion. Moreover, we should stress that the impact of the reported gains in the 3-year simulated time-frame is better understood if seen in the frame of a longer process. More specifically, reducing vaping in a class that gets closer to graduation means also less influence to the newer classes that get promoted to the high school. This implies a strong accumulation affect, provided the campaign would run for longer period.

Besides, the vaping use-case is an example of outbreak that starts from a rather low infection level. This falls in the regime where securing high degree nodes is critical due to their high virality toward healthy peers, and refined targeting decisions for other nodes are less impactful. This is exactly what the simulation results portray. However, in scenarios where the initial infection size is larger, gLRIE would have stronger effect as our earlier synthetic experiments suggest. For instance, according to related studies, the residents of nursing homes suffering from depression are reported to be often at percentages over 40% (e.g. see [48]).

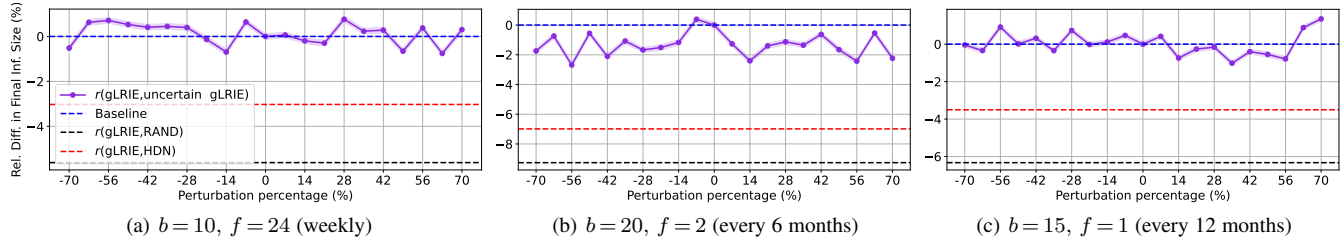


Fig. 9. Sensitivity analysis of gLRIE to parameter uncertainty in the high school vaping prevention scenario. Final relative difference in final infection size between gLRIE with the true parameters and gLRIE with uncertain parameterization is shown for varying uncertainty level considered in the latter case. Dashed lines correspond to the final relative difference between gLRIE with true parameters and its competitors. The three subfigures present different intervention scenarios in terms of budget ( $b$ ) and frequency ( $f$ ). Averaged results over 400 simulations are plotted.

## 6 CONCLUSION

In this paper we discussed a general form of recurrent two-state continuous-time Markov process that allows nonlinear node transition functions and competition among the two states that can be both diffusive. This scenario is relevant for a variety of social contagion phenomena where two opposed behaviors spread through a social network. We then proposed the *Generalized Largest Reduction in Infectious Edges* (gLRIE) algorithm which determines a greedy strategy to suppress the diffusion of the undesired state and promote the preferred one.

Synthetic experiments showed that, compared to competitors from related literature, gLRIE is well-adapted to the considered setting of competitive spreading, and makes better use of the resources available by targeting the infected nodes that are most critical for the reduction of the contagion. Finally, we illustrated the effectiveness of gLRIE in a context of a small well-monitored environment, specifically, vaping prevention in a high school social network. Comparing gLRIE with strategies that are established in real campaigns, we aimed at providing evidence on the importance of tailored interventions that account for more complex diffusion dynamics. Additionally, the multi-parameter exploration offers actionable insights for administrators who must balance intervention effectiveness with resource constraints and practical feasibility.

Future work could study more complex interaction among the epidemic states (e.g. non-exclusivity between strains), and the estimation of the diffusion functions from real data that would facilitate the application of gLRIE in practical scenarios.

## REFERENCES

[1] B. Prakash, A. Beutel, R. Rosenfeld, and C. Faloutsos, “Winner takes all: Competing viruses or ideas on fair-play networks,” in *ACM Intern. Conf. on World Wide Web*, 2012, pp. 1037–1046.

[2] J. Leskovec, L. Adamic, and B. Huberman, “The dynamics of viral marketing,” *ACM Trans. on the Web*, vol. 1, no. 1, p. 5, 2007.

[3] B. D. L. Marshall, M. M. Paczkowski, L. Seemann, B. Tempalski, E. R. Pouget, S. Galea, and S. R. Friedman, “A Complex Systems Approach to Evaluate HIV Prevention in Metropolitan Areas: Preliminary Implications for Combination Intervention Strategies,” *PLOS One*, vol. 7, no. 9, p. e44833, 2012.

[4] B. Prakash, H. Tong, N. Valler, M. Faloutsos, and C. Faloutsos, “Virus propagation on time-varying networks: Theory and immunization algorithms,” in *European Conf. on Machine Learning*, 2010, pp. 99–114.

[5] Q. Wu, H. Liu, and M. Small, “Dynamical diversity induced by individual responsive immunization,” *Physica A: Statistical Mechanics and its Applications*, vol. 392, no. 12, pp. 2792–2802, 2013.

[6] E. Valdano, C. Poletto, P.-Y. Boëlle, and V. Colizza, “Reorganization of nurse scheduling reduces the risk of healthcare associated infections,” *Scientific Reports*, vol. 11, no. 1, p. 7393, 2021.

[7] M. Fekom, N. Vayatis, and A. Kalogeratos, “Sequential dynamic resource allocation for epidemic control,” in *IEEE Conf. on Decision and Control*, 2019, pp. 6338–6343.

[8] A. Baker, I. Biazzo, A. Braunstein, G. Catania, L. Dall’Asta, A. Ingrassio, F. Krzakala, F. Mazza, M. Mézard, A. P. Muntoni, M. Refinetti, S. Sarao Mannelli, and L. Zdeborová, “Epidemic mitigation by statistical inference from contact tracing data,” *Proc. of the National Academy of Sciences*, vol. 118, no. 32, p. e2106548118, 2021.

[9] F. Jin, E. Dougherty, P. Saraf, Y. Cao, and N. Ramakrishnan, “Epidemiological modeling of news and rumors on twitter,” in *KDD Workshop on Social Network Mining and Analysis*, 2013.

[10] L. Zhu, H. Zhao, and H. Wang, “Complex dynamic behavior of a rumor propagation model with spatial-temporal diffusion terms,” *Information Sciences*, vol. 349, pp. 119–136, 2016.

[11] A. Kalogeratos, K. Scaman, L. Corinzia, and N. Vayatis, “Information diffusion and rumor spreading,” in *Cooperative and Graph Signal Processing - Chapter 24*, P. M. Djurić and C. Richard, Eds. Academic Press, 2018, pp. 651–678.

[12] G. Abel, A. Kalogeratos, J.-P. Nadal, and J. Randon-Furling, “Uncovering social network activity using joint user and topic interaction,” *Preprint arXiv.2506.12842*, 2025.

[13] H. Hu, S. Myers, V. Colizza, and A. Vespignani, “WiFi networks and malware epidemiology,” *Proc. of the National Academy of Sciences*, vol. 106, no. 5, pp. 1318–1323, 2009.

[14] A. Hill, D. Rand, M. Nowak, and N. Christakis, “Infectious disease modeling of social contagion in networks,” *PLoS Computational Biology*, vol. 6, no. 11, p. e1000968, 2010.

[15] —, “Emotions as infectious diseases in a large social network: The SISa model,” *Royal Society of London B: Biological Sciences*, vol. 277, no. 1701, pp. 3827–3835, 2010.

[16] N. Christakis and J. Fowler, “The spread of obesity in a large social network over 32 years,” *New England of Medicine*, vol. 357, no. 4, pp. 370–379, 2007.

[17] —, “The collective dynamics of smoking in a large social network,” *New England of Medicine*, vol. 358, no. 21, pp. 2249–2258, 2008.

[18] V. Verma, “Optimal control analysis of a mathematical model on smoking,” *Modeling Earth Systems and Environment*, vol. 6, pp. 2535–2542, 2020.

[19] J. Rosenquist, J. Murabito, J. Fowler, and N. Christakis, “The spread of alcohol consumption behavior in a large social network,” *Annals of Internal Medicine*, vol. 152, no. 7, pp. 426–433, 2010.

[20] E. J. Marshall, “Adolescent Alcohol Use: Risks and Consequences,” *Alcohol and Alcoholism*, vol. 49, no. 2, pp. 160–164, 2014.

[21] I. F. Hoffman, C. A. Latkin, P. V. Kukhareva, S. V. Malov, J. V. Batluk, A. V. Shabolts, R. V. Skochilov, N. V. Sokolov, S. V. Verevochkin, M. G. Hudgens, and A. P. Kozlov, “A peer-educator network HIV prevention intervention among injection drug users: Results of a randomized controlled trial in St. Petersburg, Russia,” *AIDS and Behavior*, vol. 17, no. 7, pp. 2510–2520, 2013.

[22] R. Jose, J. R. Hipp, C. T. Butts, C. Wang, and C. M. Lakon, “Network structure, influence, selection, and adolescent delinquent behavior: Unpacking a dynamic process,” *Criminal Justice and Behavior*, vol. 43, no. 2, pp. 264–284, 2016.

[23] F. Calderoni, G. M. Campedelli, A. Szekely, M. Paolucci, and G. Andrighetto, “Recruitment into organized crime: An agent-based approach testing the impact of different policies,” *Journal of Quantitative Criminology*, pp. 1–41, 2021.

[24] P. Van Mieghem, J. Omic, and R. Kooij, “Virus spread in networks,” *IEEE/ACM Trans. on Networking*, vol. 17, no. 1, pp. 1–14, 2009.

- [25] H. Hethcote, "The mathematics of infectious diseases," *SIAM Review*, vol. 42, no. 4, pp. 599–653, 2000.
- [26] M. Newman, *Networks: An Introduction*. New York, NY, USA: Oxford University Press, 2010.
- [27] V. Capasso and G. Serio, "A generalization of the Kermack-McKendrick deterministic epidemic model," *Mathematical Biosciences*, vol. 42, no. 1, pp. 43–61, 1978.
- [28] R. Campbell, F. Starkey, J. Holliday, S. Audrey, M. Bloor, N. Parry-Langdon, R. Hughes, and L. Moore, "An informal school-based peer-led intervention for smoking prevention in adolescence (ASSIST): A cluster randomised trial," *The Lancet*, vol. 371, no. 9624, pp. 1595–1602, 2008.
- [29] L. Tong, S. Zhang, H. Sun, Y. Cai, J. Zhang, W. Qian, Q. Zhang, Q. He, J. Chen, and J. Li, "Advancements in epidemic transmission suppression: A comprehensive survey," *IEEE Trans. on Network Science and Engineering*, vol. 12, no. 6, pp. 5024–5044, 2025.
- [30] H. Tong, B. A. Prakash, C. Tsourakakis, T. Eliassi-Rad, C. Faloutsos, and D. Chau, "On the vulnerability of large graphs," in *IEEE Intern. Conf. on Data Mining*, 2010, pp. 1091–1096.
- [31] S. Saha, A. Adiga, B. A. Prakash, and A. K. S. Vullikanti, "Approximation algorithms for reducing the spectral radius to control epidemic spread," in *SIAM Intern. Conf. on Data Mining*, 2015, pp. 568–576.
- [32] C. J. Kuhlman, G. Tuli, S. Swarup, M. V. Marathe, and SS. Ravi, "Blocking simple and complex contagion by edge removal," in *IEEE Intern. Conf. on Data Mining*, 2013, pp. 399–408.
- [33] K. Drakopoulos, A. Ozdaglar, and J. N. Tsitsiklis, "An efficient curing policy for epidemics on graphs," *IEEE Trans. on Network Science and Engineering*, vol. 1, no. 2, pp. 67–75, 2014.
- [34] K. Scaman, A. Kalogeratos, and N. Vayatis, "A greedy approach for dynamic control of diffusion processes in networks," in *IEEE Intern. Conf. on Tools with Artificial Intelligence*, 2015, pp. 652–659.
- [35] T. Wang, T. Liu, Y. Lu, and X. Li, "Competitive spreading model and control strategies of negative emotions and intervention information in heterogeneous social networks," *Preprint on Research Square*, 2022.
- [36] M. Lelarge, "Diffusion and cascading behavior in random networks," *Games and Economic Behavior*, vol. 75, no. 2, pp. 752–775, 2012.
- [37] E. Sadler, "Diffusion Games," *American Economic Review*, vol. 110, no. 1, pp. 225–270, 2020.
- [38] L. Cianfanelli, G. Como, F. Fagnani, A. Ozdaglar, and F. Parise, "Optimal interventions in opinion dynamics on large-scale, time-varying, random networks," *Preprint arXiv:2509.02623*, 2025.
- [39] L. Lorch, A. De, S. Bhatt, W. Trouleau, U. Upadhyay, and M. Gomez-Rodriguez, "Stochastic optimal control of epidemic processes in networks," *Preprint arXiv:1810.13043*, 2018.
- [40] K. Noorbakhsh and M. Rodriguez, "Counterfactual temporal point processes," *Advances in Neural Information Processing Systems*, vol. 35, pp. 24 810–24 823, 2022.
- [41] A. Zarezade, A. De, U. Upadhyay, H. R. Rabiee, and M. Gomez-Rodriguez, "Steering social activity: A stochastic optimal control point of view," *Journal of Machine Learning Research*, vol. 18, no. 205, pp. 1–35, 2018.
- [42] E. M. Hill, F. E. Griffiths, and T. House, "Spreading of healthy mood in adolescent social networks," *Proc. of the Royal Society B: Biological Sciences*, vol. 282, no. 1813, p. 20151180, 2015.
- [43] J. Zhang, L. Tong, P. J. Lamberson, R. A. Durazo-Arvizu, A. Luke, and D. A. Shoham, "Leveraging social influence to address overweight and obesity using agent-based models: The role of adolescent social networks," *Social Science & Medicine*, vol. 125, pp. 203–213, 2015.
- [44] A. Day, D. Newton, D. Cooke, and A. Tamatea, "Interventions to prevent prison violence: A scoping review of the available research evidence," *The Prison Journal*, vol. 102, no. 6, pp. 745–769, 2022.
- [45] M. Remch, G. Swink, C. Mautz, A. E. Austin, and R. B. Naumann, "Evaluation of a prison violence prevention program: Impacts on violent and non-violent prison infractions," *Injury Epidemiology*, vol. 10, no. 1, p. 36, 2023.
- [46] J. M. Kensbock, L. Alkærsg, and C. Lomborg, "The epidemic of mental disorders in business – How depression, anxiety, and stress spread across organizations through employee mobility," *Administrative Science Quarterly*, vol. 67, no. 1, pp. 1–48, 2022.
- [47] I. L. Abraham, M. M. Neundorfer, and L. J. Currie, "Effects of group interventions on cognition and depression in nursing home residents," *Nursing Research*, vol. 41, no. 4, p. 196, Jul. 1992.
- [48] S.-Y. Chao, H.-Y. Liu, C.-Y. Wu, S.-F. Jin, T.-L. Chu, T.-S. Huang, and M. J. Clark, "The effects of group reminiscence therapy on depression, self esteem, and life satisfaction of elderly nursing home residents," *Journal of Nursing Research*, vol. 14, no. 1, p. 36, 2006.
- [49] L. Chen, F. Ghanbarnejad, and D. Brockmann, "Fundamental properties of cooperative contagion processes," *New of Physics*, vol. 19, no. 10, p. 103041, 2017.
- [50] Z. Wang, M. Tang, S. Cai, Y. Liu, J. Zhou, and D. Han, "Self-awareness control effect of cooperative epidemics on complex networks," *Chaos*, vol. 29, no. 5, 2019.
- [51] A. Beutel, B. Prakash, R. Rosenfeld, and C. Faloutsos, "Interacting viruses in networks: Can both survive?" in *ACM SIGKDD Intern. Conf. on Knowledge Discovery and Data Mining*, 2012, pp. 426–434.
- [52] P. E. Paré, J. Liu, C. L. Beck, A. Nedić, and T. Başar, "Multi-competitive viruses over static and time-varying networks," in *American Control Conf.*, 2017, pp. 1685–1690.
- [53] L.-X. Yang, X. Yang, and Y. Y. Tang, "A bi-virus competing spreading model with generic infection rates," *IEEE Trans. on Network Science and Engineering*, vol. 5, no. 1, pp. 2–13, 2018.
- [54] J. Liu, P. E. Paré, A. Nedić, C. Y. Tang, C. L. Beck, and T. Başar, "Analysis and control of a continuous-time bi-virus model," *IEEE Intern. Conf. on Automatic Control*, vol. 64, no. 12, pp. 4891–4906, 2019.
- [55] F. D. Sahneh and C. Scoglio, "Competitive epidemic spreading over arbitrary multilayer networks," *Physical Review E*, vol. 89, no. 6, p. 062817, 2014.
- [56] R. S. Akondy, P. L. F. Johnson, H. I. Nakaya, S. Edupuganti, M. J. Mulligan, B. Lawson, J. D. Miller, B. Pulendran, R. Antia, and R. Ahmed, "Initial viral load determines the magnitude of the human cd8 t cell response to yellow fever vaccination," *Proc. of the National Academy of Sciences*, vol. 112, no. 10, pp. 3050–3055, 2015.
- [57] C. Zhang, S. Gracy, T. Başar, and P. E. Paré, "Analysis, state estimation, and control for the networked competitive multi-virus SIR model," *Automatica*, vol. 180, p. 112479, Oct. 2025.
- [58] L. Cristancho-Fajardo, P. Ezanno, and E. Vergu, "Dynamic resource allocation for controlling pathogen spread on a large metapopulation network," *Journal of the Royal Society Interface*, vol. 19, no. 188, p. 20210744, 2022.
- [59] R. Fan, K. Xu, and J. Zhao, "An agent-based model for emotion contagion and competition in online social media," *Physica A*, vol. 495, pp. 245–259, Apr. 2018.
- [60] J. G.T. and B. T.A., "The effect of friend selection on social influences in obesity," *Economics & Human Biology*, vol. 15, pp. 153–164, 2014.
- [61] A. Labzai, O. Balatif, and M. Rachik, "Optimal control strategy for a discrete time smoking model with specific saturated incidence rate," *Discrete Dynamics in Nature and Society*, vol. 2018, pp. 1–10, 2018.
- [62] P. A. Wyman, K. Rulison, A. R. Pisani, E. M. Alvaro, W. D. Crano, K. Schmeelk-Cone, C. K. Elliot, J. Wortzel, T. A. Pickering, and D. L. Espelage, "Above the influence of vaping: Peer leader influence and diffusion of a network-informed preventive intervention," *Addictive Behaviors*, vol. 113, p. 106693, 2021.
- [63] T. W. Valente, S. E. Piombo, K. M. Edwards, E. A. Waterman, and V. L. Banyard, "Social network influences on adolescent e-cigarette use," *Substance Use & Misuse*, vol. 58, no. 6, pp. 780–786, 2023.
- [64] M. Fudolig and R. Howard, "The local stability of a modified multi-strain SIR model for emerging viral strains," *PLOS One*, vol. 15, no. 12, pp. 1–27, 2020.
- [65] C. Zhang, S. Gracy, T. Başar, and P. E. Paré, "Networked competitive multi-virus SIR model," in *American Control Conf.*, 2022, pp. 3348–3348.
- [66] J. Codella, N. Safdar, R. Heffernan, and O. Alagoz, "An agent-based simulation model for Clostridium difficile infection control," *Medical Decision Making*, vol. 35, no. 2, pp. 211–229, 2015.
- [67] R. A. Nianogo and O. A. Arah, "Agent-based modeling of noncommunicable diseases: A systematic review," *American Journal of Public Health*, vol. 105, no. 3, pp. e20–e31, 2015.
- [68] M. Tracy, M. Cerdá, and K. M. Keyes, "Agent-based modeling in public health: Current applications and future directions," *Annual Review of Public Health*, vol. 39, no. 1, pp. 77–94, 2018.
- [69] R. F. Hunter, K. de la Haye, J. M. Murray, J. Badham, T. W. Valente, M. Clarke, and F. Kee, "Social network interventions for health behaviours and outcomes: A systematic review and meta-analysis," *PLoS Medicine*, vol. 16, no. 9, p. e1002890, 2019.
- [70] A. Utarini, C. Indriani, R. A. Ahmad, W. Tantowijoyo, E. Arguni, M. R. Ansari, E. Supriyati, D. S. Wardana, Y. Meitika, I. Ernesia, I. Nurhayati, E. Prabowo, B. Andari, B. R. Green, L. Hodgson, Z. Cutcher, E. Rancès, P. A. Ryan, S. L. O'Neill, S. M. Dufault, S. K. Tanamas, N. P. Jewell, K. L. Anders, and C. P. Simmons, "Efficacy of Wolbachia-infected mosquito deployments for the control of dengue," *New England of Medicine*, vol. 384, no. 23, pp. 2177–2186, 2021.
- [71] S. B. Pinto, T. I. S. Riback, G. Sylvestre, G. Costa, J. Peixoto, F. B. S. Dias, S. K. Tanamas, C. P. Simmons, S. M. Dufault, P. A. Ryan, S. L.

O'Neill, F. C. Muzzi, S. Kutcher, J. Montgomery, B. R. Green, R. Smithyman, A. Eppinghaus, V. Saraceni, B. Durovni, K. L. Anders, and L. A. Moreira, "Effectiveness of Wolbachia-infected mosquito deployments in reducing the incidence of dengue and other Aedes-borne diseases in Niterói, Brazil: A quasi-experimental study," *PLOS Neglected Tropical Diseases*, vol. 15, no. 7, pp. 1–23, 2021.

- [72] J. Zhang, L. Liu, Y. Li, and Y. Wang, "An optimal control problem for dengue transmission model with Wolbachia and vaccination," *Communications in Nonlinear Science and Numerical Simulation*, vol. 116, p. 106856, 2023.
- [73] K. Milburn, "A critical review of peer education with young people with special reference to sexual health," *Health Education Research*, vol. 10, no. 4, pp. 407–420, 1995.
- [74] T. A. Pickering, P. A. Wyman, K. Schmeelk-Cone, C. Hartley, T. W. Valente, A. R. Pisani, K. L. Rulison, C. H. Brown, and M. LoMurray, "Diffusion of a peer-led suicide preventive intervention through school-based student peer and adult networks," *Frontiers in Psychiatry*, vol. 9, 2018.
- [75] P. V. Mieghem, "The N-intertwined SIS epidemic network model," *Computing. Archives for Scientific Computing*, vol. 93, pp. 147–169, 2011.
- [76] K. Scaman, A. Kalogeratos, and N. Vayatis, "Suppressing epidemics in networks using priority planning," *IEEE Trans. on Network Science and Engineering*, vol. 3, no. 4, pp. 271–285, 2016.
- [77] L. A. Adamic and N. Glance, "The political blogosphere and the 2004 U.S. election: Divided they blog," in *LinkKDD Intern. Workshop on Link Discovery*, 2005, pp. 36–43.
- [78] G. F. Chami, S. E. Ahnert, N. B. Kabatereine, and E. M. Tukahebwa, "Social network fragmentation and community health," *Proc. of the of the National Academy of Sciences*, vol. 114, no. 36, pp. E7425–E7431, 2017.
- [79] W. Hollingworth, D. Cohen, J. Hawkins, R. A. Hughes, L. A. Moore, J. C. Holliday, S. Audrey, F. Starkey, and R. Campbell, "Reducing smoking in adolescents: Cost-effectiveness results from the cluster randomized ASSIST – A Stop Smoking In Schools Trial," *Nicotine & Tobacco Research*, vol. 14, no. 2, pp. 161–168, 2012.
- [80] D. R. S. Habib and A. Kady, "Applying social network theory to vaping in high school: Implications for person-centered intervention," *Substance Use & Misuse*, vol. 59, no. 11, pp. 1667–1671, 2024.
- [81] M. Ruiz-García, J. Ozaita, M. Pereda, A. Alfonso, P. Brañas-Garza, J. A. Cuesta, and A. Sánchez, "Triadic influence as a proxy for compatibility in social relationships," *Proc. of the National Academy of Sciences*, vol. 120, no. 13, p. e2215041120, 2023.
- [82] R. A. Miech, L. D. Johnston, M. E. Patrick, and P. M. O'Malley, "Monitoring the future national survey results on drug use, 1975-2024: Overview and key findings on secondary school students," Institute for Social Research, Tech. Rep., 2024.

## Acknowledgments

A.K. and G.A. acknowledge support from the Industrial Data Analytics and Machine Learning Chair hosted at ENS Paris-Saclay, Université Paris-Saclay. S.S.M. is supported by the Wallenberg AI, Autonomous Systems, and Software Program (WASP).

## APPENDIX

### ANALYTICAL DERIVATION OF THE GLRIE SCORE

*Proof.* Equation 4.7

Let us begin by considering the expansion, with respect to  $u$ , of the cost function introduced in Eq. 4.1:

$$\begin{aligned} Cost(\Lambda, X, \gamma) &= \int_0^\infty e^{-\gamma u} \mathbb{E}[N_I(t+u)|X(t)=X] du \\ &= \frac{1}{\gamma} \Phi_{t,X}(0) + \frac{1}{\gamma^2} \Phi'_{t,X}(0) + \frac{1}{\gamma^3} \Phi''_{t,X}(0) + O\left(\frac{1}{\gamma^4}\right), \end{aligned}$$

where  $\Phi_{t,X} = \mathbb{E}[N_I(t+u)|X(t)=X]$ .

**First order term.** This is trivial and does not contain any useful information:

$$\Phi_{t,X}(0) = \sum_i X_i.$$

**Second order term.** The derivative of a generic function  $\mathcal{F}$  is defined as:

$$\frac{\partial}{\partial t} \mathbb{E}[\mathcal{F}(t)] = \lim_{\Delta t \rightarrow 0} \frac{\mathbb{E}[\mathcal{F}(t+\Delta t)] - \mathbb{E}[\mathcal{F}(t)]}{\Delta t}.$$

The second term:

$$\begin{aligned} \Phi'_{t,X}(0) &= \left\{ \sum_i \frac{\partial}{\partial u} \mathbb{E}[X_i(t+u)|X(t)] \right\} \Big|_{u=0} \\ &= \left\{ -\sum_i \mathbb{E}[\mathcal{H}_i X_i] - \rho \sum_i \mathbb{E}[B_i X_i] + \sum_i \mathbb{E}[\mathcal{I}_i \bar{X}_i] \right\} \Big|_{u=0} \\ &= -\sum_i \mathcal{H}_i X_i - \rho \sum_i B_i X_i + \sum_i \mathcal{I}_i \bar{X}_i, \end{aligned}$$

which suggests that the treatments are effective only if applied to infected nodes, since they are curing and not preventive resources.

**Third order.** This term is a bit more complicated:

$$\begin{aligned} \Phi''_{t,X}(0) &= \sum_i \frac{\partial^2}{\partial u^2} \mathbb{E}[X_i(t+u)|X(t)] \Big|_{u=0} \\ &= -\sum_i \frac{\partial}{\partial u} \mathbb{E}[\mathcal{H}_i X_i] \Big|_{u=0} - \rho \sum_i \frac{\partial}{\partial u} \mathbb{E}[B_i X_i] \Big|_{u=0} \\ &\quad + \sum_i \frac{\partial}{\partial u} \mathbb{E}[\mathcal{I}_i \bar{X}_i] \Big|_{u=0} \end{aligned}$$

We will consider all the terms separately.

At order  $\mathcal{O}(\Delta t)$ :

$$\begin{aligned} &\mathbb{E}[\mathcal{H}_i(t+\Delta t)X_i(t+\Delta t)] \\ &= \mathbb{E} \left[ \bar{X}_i \Delta t \mathcal{I}_i \mathcal{H}_i + X_i(1-\Delta t \rho B_i) \left\{ \sum_{j \neq i} X_j (\mathcal{H}_j + \rho b_j) \mathcal{H}_i^{-j} \Delta t \right. \right. \\ &\quad \left. \left. + \prod_{j \neq i} [X_j(1-(\mathcal{H}_j + \rho b_j)\Delta t) + \bar{X}_j(1-\mathcal{I}_j \Delta t)] \mathcal{H}_i \right. \right. \\ &\quad \left. \left. + \sum_{j \neq i} \bar{X}_j \mathcal{I}_j \mathcal{H}_i^{+j} \Delta t \right\} - X_i \Delta t \left\{ \sum_{j \neq i} X_j (\mathcal{H}_j + \rho b_j) (\mathcal{H}_i^{-j})^2 \Delta t \right. \right. \\ &\quad \left. \left. + \prod_{j \neq i} [X_j(1-(\mathcal{H}_j + \rho b_j)\Delta t) + \bar{X}_j(1-\mathcal{I}_j \Delta t)] (\mathcal{H}_i)^2 \right. \right. \\ &\quad \left. \left. + \sum_{j \neq i} \bar{X}_j \mathcal{I}_j (\mathcal{H}_i^{+j})^2 \Delta t \right\} \right] + \mathcal{O}(\Delta t^2), \end{aligned}$$

where  $\mathcal{H}_i^{+j} = \mathcal{H}_i(X_1, X_2, \dots, X_j = 0, \dots, X_N)$ ,  $\mathcal{H}_i^{-j} = \mathcal{H}_i(X_1, X_2, \dots, X_j = 1, \dots, X_N)$ , and analogously for the infection function  $\mathcal{I}_i^{\pm j}$ . The result is:

$$\begin{aligned} \frac{\partial}{\partial u} \mathbb{E}[X_i \mathcal{H}_i] &= \mathbb{E} \left\{ \bar{X}_i \mathcal{I}_i \mathcal{H}_i - X_i (\rho B_i + \mathcal{H}_i) \mathcal{H}_i \right. \\ &\quad \left. + X_i \left[ -\sum_{j \neq i} (\mathcal{H}_i - \mathcal{H}_i^{-j}) X_j (\mathcal{H}_j + \rho b_j) \right. \right. \\ &\quad \left. \left. + \sum_{j \neq i} (\mathcal{H}_i^{+j} - \mathcal{H}_i) \bar{X}_j \mathcal{I}_j \right] \right\}. \end{aligned}$$

Before considering the second term, let us make a note: in a small time variation  $\Delta t$  the probability of observing  $k$  changes goes

as  $\mathcal{O}(\Delta t^k)$ . In particular, the probability of no changes and one change in the number of infected in  $\Delta t$  are:

$$\begin{aligned} \mathbb{P}[N_I(t + \Delta t) = k | N_I(t) = k] &= \prod_i [X_i(1 - (\rho B_i + \mathcal{H}_i)\Delta t) + \bar{X}_i(1 - \mathcal{I}_i\Delta t)] + \mathcal{O}(\Delta t^2) \\ &= 1 - \Delta t \sum_i [X_i(\rho B_i + \mathcal{H}_i) + \bar{X}_i\mathcal{I}_i] + \mathcal{O}(\Delta t^2) \end{aligned}$$

$$\begin{aligned} \mathbb{P}[N_I(t + \Delta t) = k + 1 | N_I(t) = k] &= \sum_i \bar{X}_i\mathcal{I}_i\Delta t \prod_{j \neq i} [X_j(1 - (\rho b_j + \mathcal{H}_j^+)\Delta t) \\ &\quad + \bar{X}_j(1 - \mathcal{I}_j^+\Delta t)] + \mathcal{O}(\Delta t^3) \\ &= \sum_i \bar{X}_i\mathcal{H}_i\Delta t \prod_{j \neq i} [1 + \mathcal{O}(\Delta t)] + \mathcal{O}(\Delta t^2) \\ &= \sum_i \bar{X}_i\mathcal{I}_i\Delta t + \mathcal{O}(\Delta t^2) \end{aligned}$$

$$\begin{aligned} \mathbb{P}[N_I(t + \Delta t) = k - 1 | N_I(t) = k] &= \sum_i X_i(\rho B_i + \mathcal{H}_i)\Delta t \prod_{j \neq i} [X_j(1 - (\rho b_j + \mathcal{H}_j^-)\Delta t) \\ &\quad + \bar{X}_j(1 - \mathcal{I}_j^-\Delta t)] + \mathcal{O}(\Delta t^3) \\ &= \sum_i X_i(\rho B_i + \mathcal{H}_i)\Delta t \prod_{j \neq i} [1 + \mathcal{O}(\Delta t)] + \mathcal{O}(\Delta t^2) \\ &= \sum_i X_i(\rho B_i + \mathcal{H}_i)\Delta t + \mathcal{O}(\Delta t^2). \end{aligned}$$

We can now consider the second term:

$$\sum_i \mathbb{E}[B_i X_i] = \mathbb{E}\left[\sum_i B_i X_i\right] = \mathbb{E}[\min(b, N_I(t))].$$

Let  $H(t) = \min(b, N_I(t))$ . Then using the previous observation:

$$\mathbb{E}[H(t + \Delta t) | H(t) > b] = b + \mathcal{O}(\Delta t^2),$$

$$\begin{aligned} \mathbb{E}[H(t + \Delta t) | H(t) = b] &= b \left\{ 1 - \Delta t \sum_i [X_i(\rho B_i + \mathcal{H}_i) + \bar{X}_i\mathcal{I}_i] \right\} \\ &\quad + (b - 1) \left\{ \sum_i X_i(\rho B_i + \mathcal{H}_i) \right\} \Delta t + \mathcal{O}(\Delta t^2) \\ &= b - \sum_i X_i(\rho B_i + \mathcal{H}_i)\Delta t + \mathcal{O}(\Delta t^2), \end{aligned}$$

$$\begin{aligned} \mathbb{E}[H(t + \Delta t) | H(t) < b] &= N_I(t) \left\{ 1 - \Delta t \sum_i [X_i(\rho B_i + \mathcal{H}_i) + \bar{X}_i\mathcal{I}_i] \right\} \\ &\quad + (N_I(t) - 1) \left\{ \sum_i X_i(\rho B_i + \mathcal{H}_i) \right\} \Delta t \\ &\quad + (N_I(t) + 1) \left\{ \sum_i \bar{X}_i\mathcal{I}_i \right\} \Delta t + \mathcal{O}(\Delta t^2) \\ &= N_I(t) - \sum_i X_i(\rho B_i + \mathcal{H}_i)\Delta t + \sum_i \bar{X}_i\mathcal{I}_i\Delta t + \mathcal{O}(\Delta t^2), \end{aligned}$$

and finally:

$$\begin{aligned} \frac{\partial}{\partial t} \mathbb{E}[H(t)] &= -\mathbb{E}\left[\mathbf{1}\{N_I(t) \leq b\} \sum_i X_i(\rho B_i + \mathcal{H}_i)\right] \\ &\quad + \mathbb{E}\left[\mathbf{1}\{N_I(t) < b\} \sum_i \bar{X}_i\mathcal{I}_i\right], \end{aligned}$$

where recall that  $\mathbf{1}\{\cdot\}$  stands for the indicator function. This new term does not bring any new information. It suggests, same as the second order term does, to apply the cure only to the infected nodes. The third term is conceptually similar to the first one, and can be split in:

$$\frac{\partial}{\partial t} \mathbb{E}[\bar{X}_i\mathcal{I}_i] = \frac{\partial}{\partial t} \mathbb{E}[\mathcal{I}_i] - \frac{\partial}{\partial t} \mathbb{E}[X_i\mathcal{I}_i],$$

$$\begin{aligned} \frac{\partial}{\partial t} \mathbb{E}[\mathcal{I}_i] &= \mathbb{E}\left[\sum_{j \neq i} \mathcal{I}_i^{+j} \bar{X}_j\mathcal{I}_j - \mathcal{I}_i \sum_{j \neq i} [\bar{X}_j\mathcal{I}_j - X_j(\rho b_j + \mathcal{H}_j)] \right. \\ &\quad \left. + \sum_{j \neq i} \mathcal{I}_i^{-j} X_j(\rho b_j + \mathcal{H}_j)\right] \\ &= \mathbb{E}\left[\sum_{j \neq i} (\mathcal{I}_i^{+j} - \mathcal{I}_i) \bar{X}_j\mathcal{I}_j - \sum_{j \neq i} (\mathcal{I}_i - \mathcal{I}_i^{-j}) X_j(\rho b_j + \mathcal{H}_j)\right], \\ \frac{\partial}{\partial t} \mathbb{E}[X_i\mathcal{I}_i] &= \mathbb{E}\left\{\bar{X}_i\mathcal{I}_i^2 - X_i(\rho B_i + \mathcal{H}_i)\mathcal{I}_i + X_i \left[ \sum_{j \neq i} (\mathcal{I}_i^{+j} - \mathcal{I}_i) \bar{X}_j\mathcal{I}_j \right. \right. \\ &\quad \left. \left. - \sum_{j \neq i} (\mathcal{I}_i - \mathcal{I}_i^{-j}) X_j(\mathcal{H}_j + \rho b_j) \right] \right\}. \end{aligned}$$

We can group in the variable  $\Xi(t)$  the terms that do not bring new information:

$$\begin{aligned} \Phi''_{t,X}(0) &= \rho \sum_i \left\{ X_i B_i (\mathcal{H}_i + \mathcal{I}_i) \right. \\ &\quad \left. + \sum_{j \neq i} [X_i(\mathcal{H}_i - \mathcal{H}_i^{-j}) - \bar{X}_i(\mathcal{I}_i - \mathcal{I}_i^{-j})] X_j b_j \right\} + \Xi(t) \\ &= \rho \left\{ \sum_i [X_i B_i (\mathcal{H}_i + \mathcal{I}_i)] \right. \\ &\quad \left. + \sum_{\substack{i,j \\ i \neq j}} [X_i(\mathcal{H}_i - \mathcal{H}_i^{-j}) - \bar{X}_i(\mathcal{I}_i - \mathcal{I}_i^{-j})] X_j b_j \right\} + \Xi(t) \\ &= \rho \left\{ \sum_i [X_i B_i (\mathcal{H}_i + \mathcal{I}_i)] \right. \\ &\quad \left. + \sum_{\substack{i,j \\ i \neq j}} [X_j(\Delta \mathcal{H}_j^{-i}) - \bar{X}_j(\Delta \mathcal{I}_j^{-i})] X_i B_i \right\} + \Xi(t) \\ &= \rho \sum_i \left\{ (\mathcal{H}_i + \mathcal{I}_i) \right. \\ &\quad \left. + \sum_{j \neq i} [X_j(\Delta \mathcal{H}_j^{-i}) - \bar{X}_j(\Delta \mathcal{I}_j^{-i})] X_i B_i \right\} + \Xi(t). \end{aligned}$$

Finally, in order to minimize the infection, our analysis suggests to heal only infected nodes and consider the score  $S_i$  according to the last term:

$$S_i = - \left[ (\mathcal{H}_i + \mathcal{I}_i) + \sum_{j \neq i} [X_j(\Delta \mathcal{H}_j^{-i}) - \bar{X}_j(\Delta \mathcal{I}_j^{-i})] \right].$$

□